

# **Determining the Effectiveness of Incorporating Geographic Information into Vehicle Performance Algorithms**

Sera White

April 2012



The INL is a U.S. Department of Energy National Laboratory  
operated by Battelle Energy Alliance

# **Determining the Effectiveness of Incorporating Geographic Information into Vehicle Performance Algorithms**

**Sera White**

**April 2012**

**Idaho National Laboratory  
Idaho Falls, Idaho 83415**

**<http://www.inl.gov>**

**Prepared for the  
U.S. Department of Energy  
Assistant Secretary for Energy Efficiency and Renewable Energy  
Under DOE Idaho Operations Office  
Contract DE-AC07-05ID14517**



Determining the Effectiveness of Incorporating Geographic Information into  
Vehicle Performance Algorithms

INL/EXT-12-25144

by

Sera White

A thesis

submitted in partial fulfillment

of the requirements for the degree of

Master of Science in Geographic Information Science

Idaho State University

Spring 2012



To the Graduate Faculty:

The members of the committee appointed to examine the thesis of Sera White find it satisfactory and recommend that it be accepted.

---

Daniel P. Ames, Ph.D.  
Major Advisor

---

David W. Rodgers, Ph.D.  
Committee Member

---

Kenneth W. Bosworth, Ph.D.  
Graduate Faculty Representative

## **Dedication**

To my husband, Greg Bosen, and my son, Avi.

## **Acknowledgements**

I would like acknowledge and thank my coworkers at the Idaho National Laboratory for providing me with direction, support, and insight. I really appreciate my committee members' patience during the completion this thesis. I am grateful and for the support of all of my friends and family.

# Table of Contents

List of Figures .....	ix
List of Tables .....	xii
Abstract .....	xiii
Chapter 1: Introduction .....	1
1.1 Problem Statement .....	4
1.2 Knowledge Gaps .....	5
1.3 Research Objectives and Hypothesis .....	6
1.4 Thesis Format .....	7
Chapter 2: Literature Relevant to Fleet-based PHEV Research .....	8
Chapter 3: Data Selection and Preparation .....	14
3.1: Sample Data Selection – Choosing a Subfleet .....	15
3.2: Comparison of Sample Fleet to All Fleets .....	16
3.3: Use NED Regions to Restrict Subfleet Data .....	21
Chapter 4: Evaluation of the Effectiveness of Incorporating Instantaneous Slope into a Plug-In Hybrid Electric Vehicle Aggressive Driving Algorithm .....	26
4.1: Two Tractive Power Equations .....	27
4.2: Obtaining Elevation and Calculating Road Grade .....	29
4.3: Converting Tractive Power to Tractive Effort .....	31
4.4: Comparison of Equation 1, Equation 2 and Experimentally obtained Tractive Effort Values .....	32
4.5: Differences between 1/3 and 1/9 Arc Second NED Data .....	41
Chapter 5: Evaluation of the Effectiveness of Incorporating Geographic Road Type into a Route Type Algorithm .....	47
5.1: Three Route Type Calculation Methods .....	48
5.2: Incorporating Geographic Road Type into Vehicle Trip Data .....	49

5.3: Comparison of Geographically determined Route Type to J2841 and AVTA route types.....	58
Chapter 6: Conclusions .....	64
6.1: Incorporating Slope into Aggressiveness Calculations .....	64
6.2: Using Geographic Road Type to Classify Route Type.....	66
6.3: Final Conclusions .....	67
Chapter 7: References .....	68
Appendices.....	72
Appendix A: C# Code used to create the User Defined Function for SQL Server .....	72
Appendix B: SQL Server T-SQL used to register the UDF .DLL File into the SQL Server Database .....	73
Appendix C: Entity Relationship Diagram for the SQL Server database used for the research presented within this thesis .....	74
Appendix D: SQL Server T-SQL used to produce the random sample of trips used within the research presented within this thesis .....	75
Appendix E: Screenshots of Various ArcMap 10 Geoprocessing Tools .....	76
Appendix F: Free Body Diagram Detailing Physics Behind Equation 1.....	78

## List of Figures

Figure 1 - Hymotion Prius PHEV equipped with an A123Systems' Hymotion L5 Conversion Module. The module is placed in the trunk of the vehicle (Stricker 2008). .....	3
Figure 2 - Picture of the V2Green Data Logging System (Green Gears 2012). .....	4
Figure 3. Map showing the distribution of the plug-in hybrid electric vehicles the AVTA researchers collected data on. The size of the circles represents the number of vehicles contained within each state. The density distribution is meant to quickly demonstrate the areas containing the highest number of vehicles. ....	15
Figure 4. Comparison of average miles driven per day between datasets. ....	17
Figure 5. Comparison of aggressive driving behavior between datasets. Aggressiveness was calculated for each trip using the length of time the vehicle's accelerator pedal was depressed more than 40%. The x-axis represents bins of aggressiveness ranges. For example, 0-10 represents non-aggressive driving and 90-100 represents extremely aggressive driving. ....	18
Figure 6. Comparison of average speed per trip between datasets. ....	19
Figure 7. Comparison of the percentage of city versus highway trips between datasets. The city and highway classifications shown in this figure were determined using an AVTA route type classification that uses average speed, number of stops and number of vehicle accelerations. ....	19
Figure 8. Map displaying the geographic extent of all trips within the subfleet. The points, over 30,000,000, represent the drive GPS data collected in the CA subfleet. The points look like lines because, at this resolution, they are too close to distinguish as points. ....	20
Figure 9. Map of the 1/9-arc second National Elevation Data availability in the state of California. ....	22
Figure 10. Process flow outlining the methodology behind obtaining trip data contained only within the NED regions. ....	23
Figure 11. SQL Server's STWITHIN function will intersect the region polygon with each point within the dataset. In this case, points 1 and 2 will return true and point 3 will return false. If points 1, 2, and 3 all belong to an individual vehicle trip, this trip would be excluded from the research. ....	25
Figure 12. Equation 3 is derived from this triangle. ....	31



Figure 13. Each trip's elevation change plotted in order of greatest elevation loss to greatest elevation gain. The trips are plotted in order along the x-axis. The red circles represent the areas that the following figures will focus on. ....33

Figure 14. Graph of tractive effort values calculated using Equation 1 of the trips exhibiting large elevation loss. The data are plotted along the x-axis by trip number ordered by elevation change. The red arrow highlights a trip that contains a steep incline that negates the large elevation loss that occurs slowly across the rest of the trip. ....35

Figure 15. Graph of tractive effort values calculated using Equation 2 of the trips exhibiting large elevation loss. The data are plotted along the x-axis by trip number ordered by elevation change. ....36

Figure 16. Graph of tractive effort values calculated using Equation 1 of the trips exhibiting large elevation gain. The data are plotted along the x-axis by trip number ordered by elevation change. ....37

Figure 17. Graph of tractive effort values calculated using Equation 2 of the trips with the greatest elevation gain. The elevation change also is graphed for reference. The data are plotted in the order of elevation loss to gain. ....38

Figure 18. Graph of tractive effort values calculated using Equation 2 of the trips consisting of little or no elevation change. The elevation change also is graphed for reference. The data are plotted in the order of elevation loss to gain. ....39

Figure 19. Graph of tractive effort values calculated using Equation 2 of trips consisting of little or no elevation change. The elevation change also is graphed for reference. The data are plotted in the order of greatest loss elevation loss to gain. ....40

Figure 20. Box and whisker chart comparing the distributions between tractive effort calculated experimentally and using Equation 2 and  $1/3$  arc second grade. 41

Figure 21. Trip 1 represents the single trip that had the greatest positive elevation change in the  $1/9$ -arc second elevation dataset. These data are plotted along the x axis starting with the first elevation point collected to the last data point collected. ....43

Figure 22. Trip 1 elevation change. This chart helps demonstrate the differences between the changes in elevation between the  $1/9$  and  $1/3$ -arc second elevation datasets. These data are plotted in the order they were collected. ....43

Figure 23. Trip 2 represents the single trip that had the greatest positive elevation change in the  $1/3$ -arc second elevation dataset. These data are plotted in the order they were collected. ....44

Figure 24. Trip 2 elevation change. This chart helps demonstrate the differences between the changes in elevation between the 1/9 and 1/3-arc second elevation datasets. These data are plotted in the order they were collected. ....	44
Figure 25. This graph shows the delta between the 1/3 and 1/9-arc second tractive effort values using both Equation 1 and Equation 2. The largest error between the two calculations occurs in trips that are less than 0.3 miles. The delta between the two tractive effort values is minimized when Equation 2 is used.....	46
Figure 26. Data flow of the highway and city geographic route type classification. ....	50
Figure 27. Provides an example of how the Clip, Buffer and Intersect geoprocessing tools create a small subset of street data. ....	52
Figure 28. Map showing a trip that was improperly classified as a city trip when the codes A63 and A64 were classified as city roads. ....	55
Figure 29. Map demonstrating a trip that includes many alley road type classifications. ....	57
Figure 30. Chart graphically displaying data showed in Table 7. ....	60
Figure 31. Map showing a trip classified as highway by the GEO algorithm, but the trip is more representative of a city trip. It shows many lower speeds along the interstate and a few stops. There are portions of the trip where the speed approaches zero. This trip occurred around 4 p.m. on a weekday, indicating the trip likely occurred during rush hour. ....	61
Figure 32. An example of J2841 possibly misclassifying a trip. The majority of the trip occurs on an interstate over fast speeds. However, there are numerous stops at the beginning of the trip that may cause the average to inaccurately reflect the route type.....	62

## List of Tables

Table 1. The Advanced Vehicle Testing Activity's accelerated test for plug-in hybrid electric vehicles (Carlson, Henning, et al. 2009).....	11
Table 2. Statistics describing the USA fleet and the CA subfleet. This study only considers data logged using the V2Green data logging system. ....	17
Table 3. Descriptive statistics of the various sources of elevation. ....	42
Table 4. Shows tractive effort results for both Trip 1 and Trip 2. In both cases, the results are counterintuitive. The results of the calculations using the elevation data that exhibit the greatest change are closest to the experimentally calculated value. ....	45
Table 5. Feature class code classifications used in this research. ....	53
Table 6. Fuel economy results for all three classification algorithms. ....	59
Table 7. Shows the delta between the miles per gallon calculations produced by the GEO algorithm and the J2841 and GEO calculations.....	59

## **Abstract**

This thesis presents a research study using one year of driving data obtained from plug-in hybrid electric vehicles (PHEV) located in Sacramento and San Francisco, California to determine the effectiveness of incorporating geographic information into vehicle performance algorithms. Sacramento and San Francisco were chosen because of the availability of high resolution (1/9 arc second) digital elevation data. First, I present a method for obtaining instantaneous road slope, given a latitude and longitude, and introduce its use into common driving intensity algorithms. I show that for trips characterized by >40m of net elevation change (from key on to key off), the use of instantaneous road slope significantly changes the results of driving intensity calculations. For trips exhibiting elevation loss, algorithms ignoring road slope overestimated driving intensity by as much as 211 Wh/mile, while for trips exhibiting elevation gain these algorithms underestimated driving intensity by as much as 333 Wh/mile. Second, I describe and test an algorithm that incorporates vehicle route type into computations of city and highway fuel economy. Route type was determined by intersecting trip GPS points with ESRI StreetMap road types and assigning each trip as either city or highway route type according to whichever road type comprised the largest distance traveled. The fuel economy results produced by the geographic classification were compared to the fuel economy results produced by algorithms that assign route type based on average speed or driving style. Most results were within 1 mile per gallon (~3%) of one another; the largest difference was 1.4 miles per gallon for charge depleting highway trips. The methods for acquiring and using geographic data introduced in this thesis will enable other vehicle technology researchers to incorporate geographic data into their research problems.



## **Chapter 1: Introduction**

The U.S. Department of Energy, Vehicle Technologies Program's Advanced Vehicle Testing Activity (AVTA) has been testing plug-in hybrid electric vehicles (PHEVs) since late 2006. Today's PHEVs are of two designs. The earliest PHEVs were hybrid electric vehicles modified, or converted, into PHEVs by third-party conversion companies. More recent PHEVs are purpose-built vehicles designed and manufactured by original equipment vehicle manufacturers. In most of the earlier PHEV conversions, an additional battery pack was installed in the hybrid electric vehicle to add all-electric range and greater electric propulsion range to the vehicle. This increased the fuel economy of the car and reduced the vehicle's use of gasoline. The additional battery was charged by connecting it to the electric grid via any grounded 110-V outlet.

Original equipment manufacturers, such as Ford and Toyota, are all individually working on producing PHEVs for commercial sale. General Motors recently released the Chevy Volt, an extended-range electric vehicle, which also is considered a PHEV by the general public. Toyota is making its Prius PHEV available in the spring of 2012. All other PHEVs currently on the road have been produced by various conversion companies. The most widely sold hybrid electric vehicle, the Toyota Prius, is the most commonly converted vehicle.

Because converted PHEVs are experimental, the vehicle conversion companies are interested in monitoring various vehicle performance parameters. They place data loggers within the vehicles to monitor both vehicle and battery performance. These data help them monitor and perfect their batteries, as well as enhance the design of the vehicle for better performance.

The Idaho National Laboratory's AVTA program has agreements in place with various PHEV conversion companies to manage data from the loggers. AVTA researchers provide un-biased information about vehicle performance to the public. They analyze PHEV fleet data and provide the vehicle drivers and fleet managers with summary reports describing vehicle performance. Additionally, they produce summary reports for the entire PHEV fleet and share these with the public. These overall summary reports are available via Idaho National Laboratory's AVTA website (<http://avt.inl.gov>).

Currently, AVTA has performed the largest PHEV data collection effort in the world. To date, they have logged approximately 500,000 trips and accumulated nearly 3,000,000 PHEV miles. The AVTA data warehouse holds over 1 billion records. The majority of these data have been collected from the Hymotion Prius PHEV equipped with an A123Systems' Hymotion L5 Conversion Module (shown in Figure 1). The conversion module is a supplemental battery system that converts the Prius into a PHEV. The module uses a lithium ion battery pack with an energy capacity of 5 kWh and is designed to double the Prius fuel efficiency for the 20 – 40 miles of charge depleting range (Iu and Smart 2009).



**Figure 1 – Hymotion Prius PHEV equipped with an A123Systems' Hymotion L5 Conversion Module. The module is placed in the trunk of the vehicle (Stricker 2008).**

Most of the data described above are logged using the V2Green data logging system. The V2Green logging system, shown in Figure 2, is capable of receiving numerous signals directly from the vehicle. It can also measure and log the vehicle charging data. Global Position System (GPS) positioning is incorporated into the logging system. The system transfers its data to a centralized data repository using cellular and Wi-Fi data transfer. Some of the signals captured by the logger are: vehicle speed, fuel consumption, accelerator and brake pedal position, engine coolant temperature, battery pack current, and battery state of charge (Iu and Smart 2009).





**Figure 2 – V2Green Data Logging System (Green Gears 2012).**

### **1.1 Problem Statement**

Alternative vehicle technology advancements mostly are driven by the requirement to decrease fuel use (Evens et al. 1976). Drivers, fleet managers, and researchers seek to increase vehicle fuel efficiency for economic purposes. Often, researchers will use vehicle route type and trip aggressiveness to explain or predict vehicle fuel consumption.

Vehicle route types are used to provide fuel consumption values in terms of city and highway mpg (miles per gallon). The Environmental Protection Agency (EPA) requires original equipment manufacturers to provide consumers with city and highway mpg values for all production vehicles. Measuring these metrics requires the use of specific dynamometer tests designed to emulate city and highway driving. Research has shown that the values produced by the EPA required tests underestimate the fuel efficiency of the Hymotion PHEV (Gondor et



al. 2009). In an effort to provide the public with accurate city and highway mpg values for the on-road Hymotion PHEV dataset, AVTA researchers have formulated an algorithm described below for classifying city and highway route types.

Driving aggressively affects fuel economy. Aggressive driving, also referred to as driving intensity, is calculated using numerous methods. The method employed by AVTA for calculating driving intensity uses data collected from dynamometer tests and expert knowledge regarding the performance characteristics of the vehicle.

Neither of the methods introduced above for calculating driving intensity or route type incorporates the use of geographic data. This thesis explores the value of using geographic information to characterize route type and aggressiveness. First, I provide a methodology for incorporating slope into two standard driving intensity calculations. Second, I show how to intersect geographic road type with second-by-second trip data to classify route type. Both of these analyses provide researchers alternative methodologies for approaching route type and aggressiveness calculations using geographic information.

## **1.2 Knowledge Gaps**

Research demonstrating the incorporation of geographic information into the two types of vehicle algorithms described above is difficult to find, as is demonstrated in the literature review in Chapter 2. Commercial vehicle data loggers started shipping loggers with GPS units circa 2006. Prior to 2006, the lack of geographic data forced many vehicle researchers to identify alternative ways to characterize vehicle performance. To date, AVTA researchers have not

had the knowledge to incorporate geographic data into any of their various vehicle performance algorithms.

### **1.3 Research Objectives and Hypothesis**

The primary research objectives of this study are to provide a methodology for the incorporation of geographic information into vehicle performance algorithms and to show how the incorporation of a geographic data component can significantly improve the more general science of vehicle design.

More specifically, this thesis will address the following two hypotheses:

**Hypothesis 1:** The incorporation of road grade significantly changes the results of driving intensity calculations.

**Hypothesis 2:** It is possible to accurately classify the vehicle route type by only considering the geographic road type of the trip.

The process of testing the two hypotheses will provide the following contributions to AVTA researchers and to the overall science of advanced vehicle technology testing and design:

- Enable AVTA researchers to incorporate geographic data into algorithms that contain a geographic component.
- Provide other researchers with a methodology for incorporating geographic data into their research problems.
- Compare the results of two general tractive effort calculations to the results of experimentally obtained tractive effort values.
- Provide and test a method for obtaining road slope given latitude and longitude.

- Provide and test a method for determining a vehicle route type using geographic road data.
- Provide and test a method for obtaining a geographic road type using vehicle latitude and longitude data.

#### **1.4 Thesis Format**

The remainder of this thesis is organized as follows: In Chapter 2, I present the relevant existing research that has been conducted over the past 45 years. Chapter 3 describes my selection process for the sample dataset used throughout the research discussed within this thesis. The research and results produced by incorporating instantaneous slope into standard aggressiveness algorithms is presented in Chapter 4. Chapter 5 discusses the results and research produced by using geographic road type to classify vehicle route type. The findings and conclusions are discussed within Chapter 6. Lastly, the Appendix contains additional helpful information not presented within this thesis. This thesis uses both English and Metric units. The units I refer to throughout the thesis are industry standard units and are commonly used within research performed on various vehicle technologies.

## **Chapter 2: Literature Relevant to Fleet-based PHEV Research**

PHEV technology is a relatively new research area; therefore, published literature in the area of fleet-based research is very sparse. The U.S. Department of Energy's AVTA performs most fleet-based research. The public, vehicle technology researchers, fleet managers, fleet drivers and original equipment manufacturers (such as General Motors, Ford, and Toyota) are interested in the results generated by AVTA tests of various emerging PHEV technologies.

AVTA's light-duty PHEV testing research is performed by the Idaho National Laboratory in coordination with Electric Transportation Engineering Corporation. AVTA performs test track and dynamometer testing, as well as on-road testing. AVTA has collected vehicle data from 270 PHEVs in various types of fleets in 23 U.S. states and Canadian provinces. The research focuses on vehicle energy consumption and charging infrastructure requirements (Smart et al. 2009). Among the many factors that can influence energy consumption are outside air temperature, route type, use of air conditioning or heaters, age of the vehicle, and driving aggressiveness (Iu and Smart 2009).

Driver aggressiveness, also referred to as driving intensity, plays a large role in vehicle fuel efficiency. Nam et al. (2003) stated that "Aggressive driving produces significantly more emissions" (Nam et al. 2003). A publication produced by the EPA states that "Fuel economy has an inverse relationship to tailpipe CO<sub>2</sub> emissions" (Office of Transportation and Air Quality 2010). Carlson et al. (2007) determined that the relationship between driving aggressiveness and fuel consumption is nearly linear; as driving aggressiveness increases so does fuel

consumption (Carlson et al. 2007). There are multiple ways to calculate driver aggressiveness.

Carlson et al. (2007) defines aggressiveness as, “the energy at the wheels required for propulsion typically reported in terms of watt-hours per mile. The greater the vehicle acceleration or the faster the overall vehicle speed, then the greater the driving intensity” (Carlson et al. 2007).

Another indicator of aggressiveness is the accelerator pedal position. Iu and Smart (2009) determined, using qualitative observations of the data, that if the accelerator pedal is depressed past 40%, the Hymotion PHEV gasoline engine turns on. Otherwise, the vehicle is coasting or operating on electric propulsion only. Aggressiveness can be calculated by finding the proportion of the trip where the pedal position is greater than 40% and is then expressed as a percentage of the trip (Iu and Smart 2009).

Lindenmaier et al. (2009) suggests that instantaneous road slope should be not be ignored in aggressiveness calculations. Altitude and speed can be used to calculate the slope or grade along which the vehicle is traveling. He states that “the slope force has a strong influence on the fuel consumption especially for heavy cars and cannot be neglected.” In his research, he suggests using Shuttle Radio Topography Mission (SRTM) data to acquire altitude (Lindenmaier et al. 2009).

Research performed by Argonne National Laboratory suggested that PHEV vehicle design should be influenced by the drive cycles in which it is intended to be driven. Hymotion PHEVs are sensitive to aggressive driving because they are unable to meet the power demands of aggressive drive cycles



while using their additional battery pack. The extended battery pack is what makes the PHEV more efficient than an HEV. The Argonne researchers suggested using certain dynamometer tests, designed to exhibit aggressiveness, to design the vehicle to operate more effectively under real world driving conditions (Kwon et al. 2008).

Route type (i.e., city [urban] or highway) also heavily influences the fuel economy of a vehicle trip. Early research conducted at General Motors investigated the effects of seventeen variables on fuel consumption. Some of these include average trip speed, largest single acceleration, largest single deceleration, average trip time per unit distance, and the number of vehicle stops. The research found that fuel consumption for city routes could be estimated using average distance and average travel time (Evens et al. 1976).

AVTA researchers created an On-Road Accelerated Performance Test Program that is comprised of 5,440 miles of on-road data. This test was designed to produce repeatable on-road test results. Dedicated drivers followed repeated urban and highway driving routes on public roads. Drive cycles included combinations of urban and highway loops and range from 10 to 200 miles (Smart et al. 2009). Table 1 shows the on-road accelerated testing procedure's experimental design. For example, the first row describes one test that occurred over ten urban miles and was performed sixty times to provide a total of six hundred miles. Between each trip, described in the first row, the vehicle was charged for four hours. The results of this testing showed that the Hymotion Prius PHEV trip fuel economy decreased as trip distances increased (Francfort et al. 2009).

**Table 1. The Advanced Vehicle Testing Activity’s accelerated test for plug-in hybrid electric vehicles. The table describes the experimental design of the accelerated test. Each row describes a particular test performed by the drivers (Carlson et al. 2009).**

<b>Cycle (mi)</b>	<b>Urban (10 mi)</b>	<b>Highway (10 mi)</b>	<b>Charge (hr)</b>	<b>Reps (N)</b>	<b>Total (mi)</b>
10	1	0	4	60	600
20	1	1	8	30	600
40	4	0	12	15	600
40	2	2	12	15	600
40	0	4	12	15	600
60	2	4	12	10	600
80	2	6	12	8	640
100	2	8	12	6	600
200	2	18	12	3	600
<b>Total</b>	<b>2,340</b>	<b>3,100</b>	<b>1,344</b>	<b>162</b>	<b>5,440</b>
<b>Average</b>	<b>43%</b>	<b>57%</b>	<b>8.3</b>	<b>18</b>	

There are few papers that describe software solutions allowing vehicle researchers to visualize the geographic component of vehicle data. This capability has been shown to provide value to vehicle technology researchers. Daimler AG (formerly Daimler Chrysler) created a geographic visualization tool using MathWorks Matlab for their fleet of hydrogen fuel cell vehicles located worldwide. The tool provided them with numerous research capabilities. They used it to diagnose error messages transmitted from the vehicle. The tool was also used to help plan their hydrogen refueling station infrastructure. They were able to evaluate driving patterns across various geographic locations. They performed a pedal-position analysis that showed northern Californians drive much more aggressively than Singaporeans. They used this knowledge to optimize their control strategies and powertrains for various geographic regions. The development of this tool created multiple requests from Daimler managers and

engineers, allowing them to provide various stakeholders with quick analysis of an otherwise complicated dataset (McGuire et al. 2008).

Advanced vehicle technology research is moving towards the concept of using geographic data in vehicle control systems to enhance vehicle performance and increase fuel efficiency. Moran et al. (2010) investigated the concept of a networked PHEV vehicle. Through the use of map-based predictive technology, a vehicle could adapt its power controls to be more efficient using road terrain and traffic control data. The research suggested that digital map information could provide an energy savings of 25%. Eco-routing is one of the methods for obtaining this energy savings and maximizes vehicle trip efficiency by suggesting routes that minimize stops caused by traffic controls and traffic conditions. Eco-routes are also designed to avoid routes that may cause frequent braking or severe road inclines and declines. Predictive powertrain control will increase energy savings. This method uses elevation data to add predictive intelligence to automatic transmission shift timing enabling engineers to optimize gear selection for terrain-induced torque demands; anticipating the upcoming changes in road slope will enable more sophisticated engine control algorithms (Moran et al. 2010).

Department of Energy Laboratory researchers dominate most of the PHEV research performed today. Most PHEV data available is obtained from expensive experimentally converted vehicles. The body of research will grow as commercially available PHEV vehicles are introduced to the market. This literature review demonstrates that research incorporating geographic data into PHEV vehicle technology research is sparse. This is due to the fact that mass



produced commercially available vehicle data logging systems only started incorporating the ability to collect latitude and longitude data in 2006. As of 2012, most commercially available vehicle logging systems are incorporating this capability and future research will likely include more geographic information.

### **Chapter 3: Data Selection and Preparation**

This chapter describes the selection of a sample dataset to be used in the research described within Chapters 4 and 5. It also describes a methodology for obtaining elevation data from the USGS. The vehicle trip data used within this thesis was obtained from the AVTA Hymotion PHEV Prius data collection effort described in Chapters 1 & 2. The dataset contains over a billion records making it too large to consider in its entirety. The size of the entire dataset necessitated choosing a smaller subset of data to use for my research.

The Hymotion PHEV data collection effort was voluntary and subject to fleet owner involvement. Sixty-eight different fleets of vehicles located across the U.S. participated in the project over differing lengths of time. A map showing the distribution of vehicles across the U.S. is shown in Figure 3. The fleets contained within the dataset consisted of both public and private entities such as universities, utility companies, state governments, and city governments.

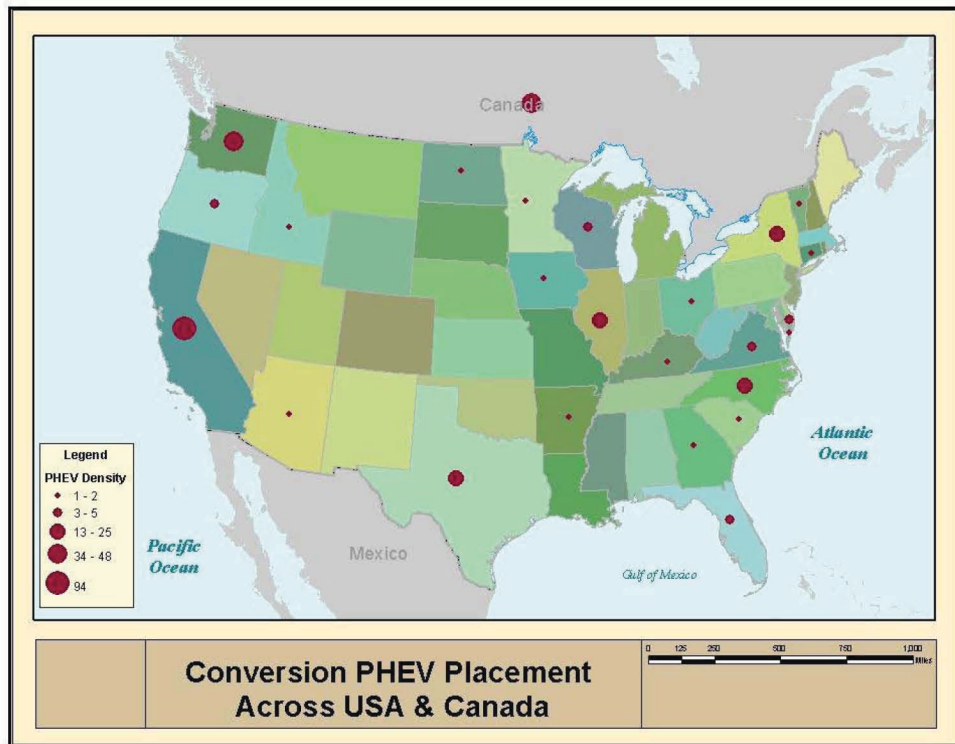


**Figure 3. Distribution of the plug-in hybrid electric vehicles that participated in the AVTA data collection effort. The size of the circles represents the number of vehicles contained within each state. The density distribution is meant to quickly demonstrate the areas containing the highest number of vehicles.**

### 3.1: Sample Data Selection – Choosing a Subfleet

Because this research uses geographic data, geographic location was a large factor in sample fleet selection. The research presented in Chapter 4 determines the necessity of using elevation obtained from either 1/3 or 1/9 arc second National Elevation Data (NED). Section 3.3 describes NED in greater detail and explains the differences between 1/3 and 1/9 arc second NED data. There are only few areas that contain 1/9 arc second data within the US, two of which are Sacramento and San Francisco.

I chose to use a fleet based within Sacramento and San Francisco. To protect the data partners within the project, I am not allowed to reveal the fleet

owner or its purpose. The data collected for the fleet spanned more than 1 year and were significantly large in comparison to other fleets within the dataset. Most of the fleets' vehicle travel occurred within the Sacramento and San Francisco areas. San Francisco's geography was ideal because it is known for its steep roads. I chose an area that exhibited large elevation gains and losses to show how aggressiveness is affected by extreme elevation change. Sacramento's low elevation variability makes it a good alternative geographic location because it provides many examples of trips not exhibiting large elevation change. These two varying types of topographies help ensure that my research considers both extremes.

### **3.2: Comparison of Sample Fleet to All Fleets**

The following section describes the statistical differences between the CA Subfleet and the USA subfleet. This analysis shows how representative the chosen subfleet is of the overall fleet. First, I produced some descriptive statistics for both the nationwide dataset (referred herein as USA fleet) and the chosen California subset (herein referred to as CA subfleet). These statistics can be viewed in Table 2. They demonstrate that the fleet of vehicles I selected consists of nearly 19% of the total miles driven and 20% of the vehicles contained in the overall data collection. It also shows that the CA subfleet only comprises 6% of the total number of vehicle trips. This suggests that the CA subfleet contains longer trips than those within the USA fleet as shown in Figure 4. To understand how representative the two fleets were, I performed two tailed paired t-tests on data shown in Figure 5 and Figure 6 (GraphPad Software 2005). The t-tests showed that the differences between the two datasets were not statistically

significant. T-tests could not be performed on Figure 4 and Figure 7 because they do not have distributions that are approximately Gaussian.

**Table 2. Statistics describing the USA fleet and the CA subfleet. This study only considers data logged using the V2Green data logging system.**

Identifier	Description	Minimum Date	Maximum Date	Total Number Vehicles	Total Driving Events	Total Miles Driven
USA fleet	All data logged (V2Green)	1/3/2008	1/31/2011	183	484,515	2,200,925
CA subfleet	Chosen subfleet for study	10/23/2009	1/31/2011	33	28,991	407,132

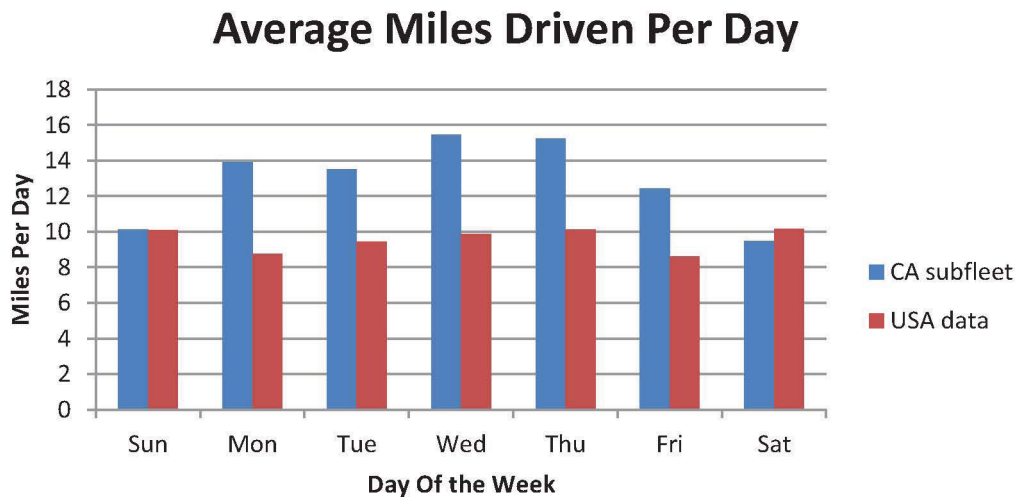


**Figure 4. Comparison of average miles driven per day between datasets.**

All of the classifications shown in Figure 5, Figure 6 and Figure 7 use the values that were used to produce the final report detailing the performance of the U.S. Hymotion PHEV fleet (Idaho National Laboratory Advanced Vehicle Testing Activity 2011). The aggressiveness values shown in Figure 5 were calculated by examining the amount of time the accelerator pedal position was depressed more than 40%. Figure 5 shows that the aggressiveness values of the CA subfleet are close to the aggressiveness values of the overall fleet. It is

important to note the terms aggressiveness and driving intensity are interchangeable. The definition of driving intensity is provided in Chapter 2. Figure 6 shows that the speeds of the CA subfleet are slightly higher than the speeds of the USA fleet. This indicates that more driving was done on highways. Figure 7 compares the percentage of city and highway trips between both datasets. The route types, city and highway, were calculated using an algorithm formulated by AVTA researchers that uses average speed, the number of stops and the number of accelerations to classify each trip. This analysis indicates that although the CA subfleet is driven differently than the entire fleet, the differences are not substantial.

## Trip Aggressiveness

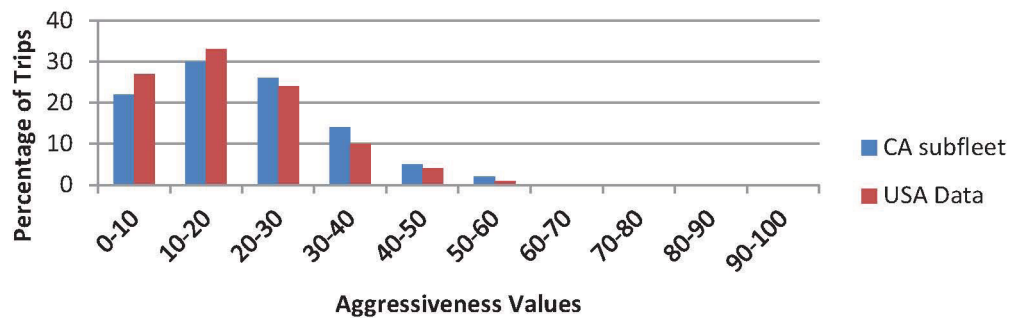


**Figure 5. Comparison of aggressive driving behavior between datasets.** Aggressiveness was calculated for each trip using the length of time the vehicle's accelerator pedal was depressed more than 40%. The x-axis represents bins of aggressiveness ranges. For example, 0-10 represents non-aggressive driving and 90-100 represents extremely aggressive driving.



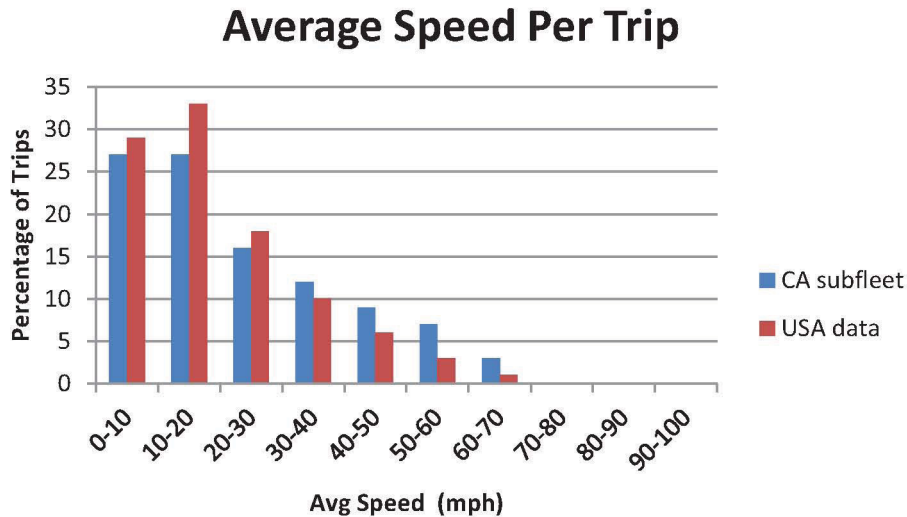


**Figure 6. Comparison of average speed per trip between datasets.**

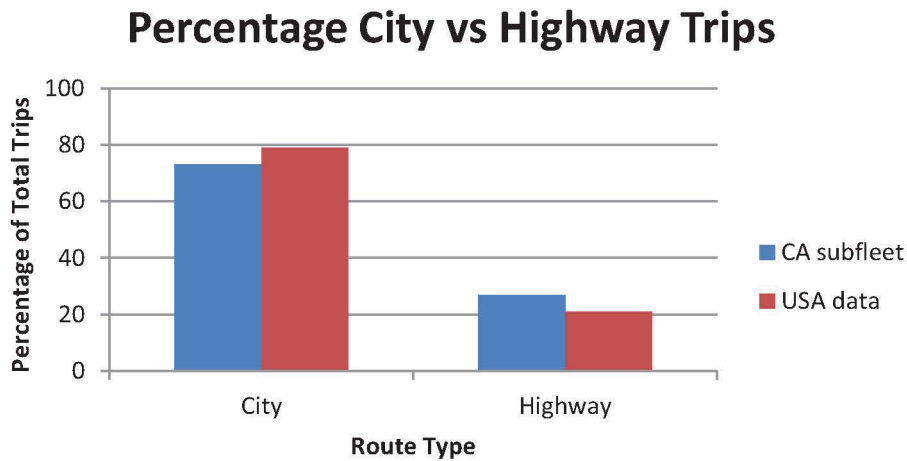


**Figure 7. Comparison of the percentage of city versus highway trips between datasets. The city and highway classifications shown in this figure were determined using an AVTA route type classification that uses average speed, number of stops and number of vehicle accelerations.**

Figure 8 shows all GPS points collected for the CA subfleet. The purpose of this figure is to show that the extent of CA subfleet data spans most of California. It also shows that there is a strong representation of trips within the cities of Sacramento and San Francisco.



**Figure 8. Geographic extent of all trips within the subfleet. The points, over 30,000,000, represent the drive GPS data collected in the CA subfleet. The points appear as lines because, at this resolution, they are too close to distinguish as points.**



### **3.3: Use NED Regions to Restrict Subfleet Data**

Once I selected a vehicle subfleet, I restricted the subfleet data to the regions that contained 1/9 arc second NED (National Elevation Dataset) data. The USGS states that “NED is the primary elevation data product of the USGS (United States Geological Survey 2010)”. NED is derived from high-resolution digital elevation data and is updated bimonthly using the newest available digital elevation models. The USGS provides NED in resolutions of 1 arc second grid cells (approximately 30 meter), 1/3 arc second grid cells (approximately 10 meters), and 1/9 arc second grid cells (approximately 3 meters). NED can be downloaded for free using the Seamless Data Warehouse (United States Geological Survey 2010). The Seamless Data Warehouse provides various web services and internet mapping applications for downloading USGS data.

Digital elevation models, such as NED, are very useful in research that uses elevation, slope, and aspect because they provide elevations in geographically referenced electronic format. Most geographic information software packages are capable of viewing and analyzing NED data. Possible research areas that may use NEDs are geologic modeling and three-dimensional visualization. Various industries (such as urban planners, emergency responders, and communications companies) use NED (United States Geological Survey 2010). Figure 9 shows the areas in which high resolution NED are available for the California region.

### 1/9 Arc Second (~3m) National Elevation Data Coverage



**Figure 9. Map of the 1/9-arc second National Elevation Data availability in the state of California.**

Figure 10 depicts the process I used to restrict the research dataset to trips contained wholly within the two NED regions show in Figure 9. Initially I used ESRI ArcMap 10, a computer mapping software package, to subset the data. The data analysis and mapping tools, provided by ArcMap, failed to effectively process approximately thirty-six million records contained within the CA subfleet. The tools would not complete execution after they were started; this is likely due

to an insufficient number of processors and insufficient amount of RAM available on the computer I used to perform the analysis.

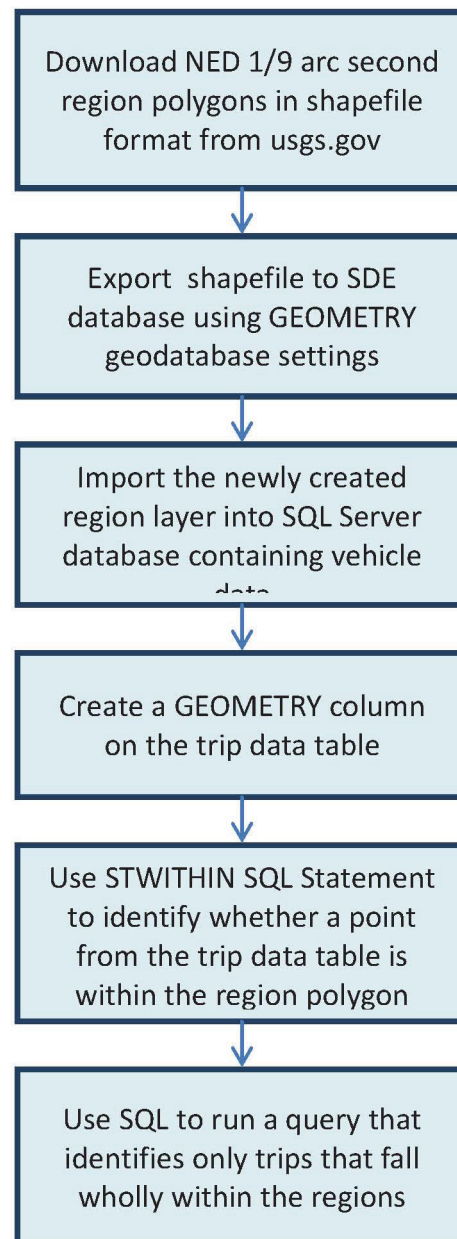


**Figure 10. Process flow outlining the methodology behind obtaining trip data contained only within the NED regions.**

Microsoft SQL Server is designed and optimized for working with large datasets. Therefore, an approach using SQL Server was developed to subset the data. The NED 1/9-arc second region polygons in shapefile format were obtained

from the USGS website (<http://usgs.gov>). The region shapefile was exported to an ESRI ArcGIS geodatabase, stored in SQL Server, using ArcGIS's Export geoprocessing tool. A geodatabase is a data repository used to store and manage spatial data and is implemented by using a relational database management system (Arctur and Zeiler 2004).

SQL Server provides the ability to perform spatial queries on data columns defined using spatial data types. Spatial data types enable SQL Server users to manage location-aware data (Fang et al. 2008). The spatial data type used by this research was GEOMETRY. The ArcMap Export tool has the capability to export the geometry of features into table with a column containing data of type GEOMETRY. Next, I imported the table from the geodatabase into the SQL Server database containing the vehicle trip data.

I defined a column of type GEOMETRY within the vehicle trip data table using latitude and longitude. Next I used SQL Server's spatial query statement STWITHIN to determine whether each data point fell inside or outside the NED region. STWITHIN determines if the geometry of one feature is contained within the geometry of another; Figure 11 provides an example. Suppose that the points 1, 2 and 3 represent a trip and the polygon represents the NED region. The STWITHIN function would determine that points 1 and 2 fall within the region and point 3 falls outside the region. Last, an SQL (Standard Query Language) statement was used to determine which trips fell wholly within the regions. The example trip shown in Figure 11 would be excluded from the research because it contains points falling outside of the region.

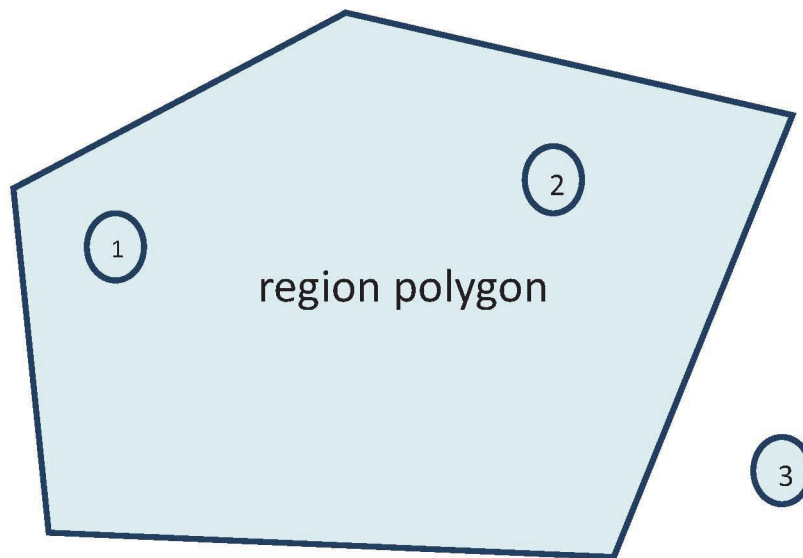


**Figure 11. SQL Server’s STWITHIN function intersects the region polygon with each point within the dataset. In this case, points 1 and 2 will return true and point 3 will return false. If points 1, 2, and 3 all belong to an individual vehicle trip, this trip would be excluded from the research.**

The resulting dataset was still very large (approximately 10,000,000 records and 15,000 trips). Simple random sampling is often used when sampling the entire dataset is unnecessary or when it is too computationally expensive (Olken and Rotem 1986). To narrow the size of the research dataset further, I used simple random sampling without replacement to produce a sample population that would represent the whole population with a 99% confidence level and a confidence interval of 3 (Stat Trek 2012). I calculated that I would need a random sample containing data from 1,647 trips. This simplified the dataset size from about 10 million records to about 1 million records. I used this subset for both of the analyses discussed within Chapters 4 and 5.



## **Chapter 4: Evaluation of the Effectiveness of Incorporating Instantaneous Slope into a Plug-In Hybrid Electric Vehicle Aggressive Driving Algorithm**

Driving intensity, also referred to as aggressiveness, affects fuel consumption. Vehicles with high-efficiency powertrains, such as hybrid electric vehicles and PHEVs, are more impacted by driving intensity. A study performed by AVTA, using PHEV dynamometer data, showed that driving intensity and fuel consumption increased nearly linearly (Carlson et al. 2009).

Carlson et al. (2010) states that mountainous driving up and down steep grades also can have a significant impact (Carlson et al. 2010). One geographical information system study showed that “driving behavior is critical for emission; lowering non-aggressive driving while going uphill would reduce emission significantly (determined via geographical information system)” (Gumusay et al. 2008). Most research on aggressive driving assumes that the slope of the road is zero. This is most likely due to the fact that slope is not always easy to obtain.

Vehicle engineers use the tractive effort, also called tractive force, at the wheel to measure driving intensity. Tractive effort is the “pushing force exerted by the vehicle’s driving wheels against the road’s surface (AutoZone 2012)”.

Driving intensity can be used to model fuel emissions, vehicle design, and fuel economy. There are numerous methods used for calculating driving intensity. AVTA researchers used response surface modeling on experimentally collected data to produce a tractive force value given a pedal position and speed. The data used to create the response surface model were collected using a dynamometer and instrumentation that recorded the exact tractive force at the wheel with varying driving intensities (Duoba et al. 2009).



#### 4.1: Two Tractive Power Equations

Tractive effort is a force that is calculated from instantaneous power.

There are two general tractive power calculations. One method uses the physical relationship between the vehicle and the road to calculate tractive effort. The second method uses dynamometer coastdown coefficients, also called dynamometer ABCs, and vehicle speed. Production vehicle dynamometer ABCs are publicly available via EPA's certification database.

The two tractive effort calculations used in this research are derived from formulas used in EPA's fuel consumption model the Physical Emission Rate Estimator (PERE) (Nam and Giannelli 2005). Both equations produce instantaneous tractive power. The first equation (Equation 1) uses common road-load methodology. It models a second-by-second drive cycle and outputs the instantaneous tractive power at each data point. Inertia, road grade, tire friction, and aerodynamic loss are all factors in Equation 1. For a more detailed breakdown and free body diagram describing Equation 1 see Appendix F.

$$P_T = mv[a(1 + \varepsilon) + g(\text{grade}) + gC_R] + 0.5\rho C_D A_F v^3 \quad \text{(Equation 1)}$$

where

$P_T$  = tractive power (Watts)

$v$  = vehicle speed (m/s)

$m$  = the mass of the vehicle (kg)

$a$  = vehicle acceleration (m/s<sup>2</sup>)

$\varepsilon$  = mass factor accounting for the rotational masses (about 0.1)

$g$  = acceleration due to gravity (9.81 m/s<sup>2</sup>)

$\text{grade}$  = road grade (generally assumed to be 0)

$C_R$  = rolling resistance (about 0.009)

$\rho$  = air density (about 1.2 kg/m<sup>3</sup>)

$C_D$  = aerodynamic drag coefficient

$A_F$  = frontal area of the vehicle (m<sup>2</sup>).

The values for coefficient of drag,  $C_D$ , and frontal area,  $A_F$ , were obtained from EPA's PERE model (Nam and Giannelli 2005). The Toyota Prius has a coefficient of drag of 0.26 and a frontal area of 2.33 m<sup>2</sup>. The mass of the converted Hymotion Prius is 1,547 kilograms. This research holds  $\epsilon$  and  $C_R$  constant. It is important to note that  $\epsilon$  has been shown to increase at lower gears and the rolling resistance,  $C_R$ , is dependent on speed, tire inflation, ground surface, and temperature. This research does not attempt to study the effects of these terms.

The second equation (Equation 2) uses the dynamometer coastdown coefficients A, B, and C and is shown below. A, B, and C are all determined using track coastdown tests and are available for certified light duty vehicles from the EPA certification database. This equation is much simpler to apply than Equation 1 and EPA states that it is preferable to Equation 1 (Nam and Giannelli 2005). A represents the rolling coefficient, B represents the rotating coefficient, and C represents aerodynamic resistance.

$$P_T = Av + Bv^2 + Cv^3 + mv[a + g(\text{grade})] \quad \text{(Equation 2)}$$

where

$P_T$  = tractive power

$A$  = coastdown coefficient, rolling coefficient

$B$  = coastdown coefficient, rotating coefficient

$C$  = coastdown coefficient, aerodynamic resistance

$v$  = vehicle velocity (m/s)

$a$  = vehicle acceleration (m/s<sup>2</sup>)

$g$  = acceleration due to gravity (9.81 m/s<sup>2</sup>)

$grade$  = road grade (generally assumed to be 0).

Both Equations 1 and 2 can be used to calculate instantaneous tractive power. Equation 2 is simpler to apply because it consists of fewer unit conversions and the coefficients are easier to obtain than those in Equation 1.

#### 4.2: Obtaining Elevation and Calculating Road Grade

Road grade is calculated using vehicle speed and elevation. I used Microsoft C# to create a DLL file that accepts a latitude and longitude and returns the associated elevation from the USGS NED web service ([http://seamless.usgs.gov/service\\_description\\_elevation.php](http://seamless.usgs.gov/service_description_elevation.php)). DLLs contain functions and resources that are compiled into executable files allowing programs running in a Windows environment to share code and resources (Microsoft 2011). Next I registered the DLL to a Microsoft SQL server user defined function. User defined functions can be called directly within a SQL query, allowing the data returned from the web service to automatically populate the database. An example call of the user defined function is shown as follows:

```
Select * From dbo.GetAllElevations(@longitude,@latitude, 'METERS',  
'ELEV*', 'True')
```

I calculated that this process would take 5 days to complete using only one process. To increase the speed of the process, I designed it to run in 10 parallel processes. I broke up the data among ten separate tables and created 10 individual processes that would use data from each table to call the user defined

function. After the process finished, I joined all of the data from the ten tables back into one table using SQL. Parallelizing the process increased the speed tenfold. Overall, the user defined function was called approximately 2 million times; it collected both a 1/3-arc second elevation and a 1/9-arc second elevation for each latitude and longitude.

This process detailed above is designed to be fully automated and deployed within the AVTA production data warehouse. Most operations involving millions of records are highly complex and take a lot of time to complete. Because of this complexity, we process AVTA data as it is loaded. The process performs quickly on small datasets and is completely encompassed within SQL Server providing the ability for complete automation. Automation eliminates the introduction of user error into the data warehouse. User error can be very difficult to find and fix.

USGS does not provide an automated interface for retrieving the 1/9 arc second NED dataset. One process for obtaining the dataset requires a user to manually download the data and merge it into one dataset using a geographic information software package. Alternatively, they will provide all of the data using an external hard drive provided by the requester. However, this process requires a great deal of time because the requestor must wait to receive the data. Once the data has been received it must be processed, managed, and maintained. This process does not guarantee that the dataset will contain the most current data because USGS updates the NEDs bimonthly (United States Geological Survey 2010). The speed of retrieval for elevations from the web service using a user

defined function is far preferable to the complexity and cost of acquiring and maintaining the entire NED dataset for the region.

After the elevation data were populated, road grade was calculated. Road grade is defined as the rise over the run or more specifically as the vertical distance divided by the horizontal distance (Gillespie 1992). The dataset already contained the distance traveled between each point. The rise is calculated by obtaining the change in elevation between points. Equation 3, based on Pythagorean's Theorem, was used to calculate the run. The triangle the equations are derived from is shown in Figure 12. The grade was calculated, for both 1/3 and 1/9 arc second elevations, by dividing the rise by the run. The grade obtained from Equation 3 is only as accurate as the data that are used within the equation. Each resolution, both 1/9 and 1/3 arc second, may produce different results for grade at the same data point. Also, an inaccurate grade will be produced if a GPS fails to transmit data for a significant portion of time.

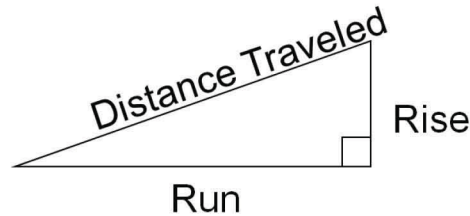


**Figure 12. Equation 3 is derived from this triangle.**

$$Run = \sqrt{(distance)^2 - (rise)^2} \quad \text{(Equation 3)}$$

#### **4.3: Converting Tractive Power to Tractive Effort**

I used Microsoft SQL server used to perform both of the tractive power calculations described in Equations 1 and 2. Tractive effort produced by the



response surface model is provided in Watt hours per mile (Wh/mi). I converted the instantaneous tractive power values produced by Equation 1 and Equation 2 to tractive effort using the following equation:

$$W = \int P_T dt$$

$$W = T_E d$$

$$T_E = \frac{W}{d} \quad \text{(Equation 4)}$$

where

$W = \text{work}$

$P_T = \text{tractive power (Watts)}$

$T_E = \text{tractive effort (Wh/mi)}$

$d = \text{distance (mi)}$ .

#### 4.4: Comparison of Equation 1, Equation 2 and Experimentally obtained Tractive Effort Values

Equation 1 and Equation 2 were used to calculate tractive effort, using road grades calculated from both 1/3 and 1/9-arc second data. The results of these calculations show that tractive effort calculations that do not consider road grade overestimate tractive effort for trips with large elevation loss and underestimate tractive effort for trips with large elevation gain. The calculated tractive effort using road grade is close to the experimentally obtained values on trips that have little elevation gain or loss.

The following group of figures demonstrates that in order to accurately characterize driving intensity in vehicle trips it is necessary to incorporate instantaneous road slope in tractive effort calculations. For simplicity the following figures only show the results of the calculations that used 1/3 arc second

elevation data. Figure 13 shows the elevation change occurring in all 1647 trips contained within the CA subfleet. The data are plotted by trip number and ordered by elevation change in each trip. The red circles on the figure show the areas that I focus on in the following groups of figures. I chose to highlight the areas exhibiting large elevation loss and gain and for contrast an area that shows little or no elevation change.

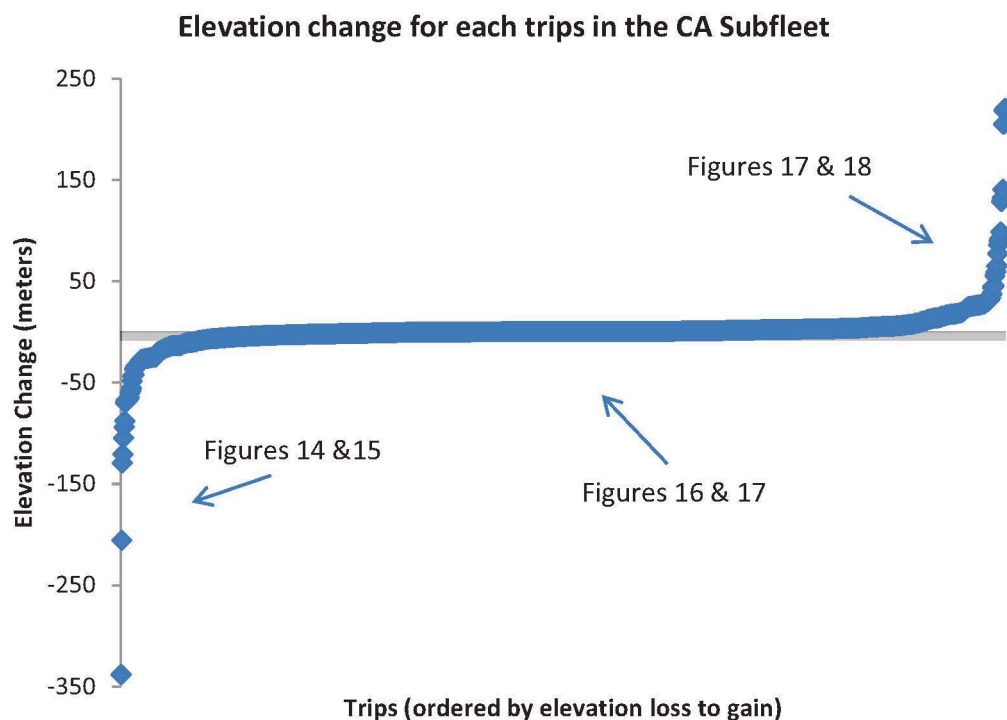


**Figure 13. Each trip's elevation change plotted in order of greatest elevation loss to greatest elevation gain. The trips are plotted in order along the x-axis. The red circles represent the areas that the following figures will focus on.**

Figure 14, graphs the trips exhibiting the largest elevation loss and shows that the larger the elevation loss the greater the difference between the various calculations. The purple dashes represent the experimentally obtained values of each trip. The blue squares represent the tractive effort value obtained from Equation 1 using  $1/3$  arc second grade. The pink squares represent the tractive

effort obtained from Equation 1 using grade equal to zero. The lines between the tractive effort points are included to help distinguish the various tractive effort values from each other.

The figure shows that the tractive efforts calculated using no grade produce similar values to the experimentally obtained tractive effort. The left side of the figure shows that experimentally obtained tractive effort values in trips exhibiting large elevation loss are generally overestimated. The right side of the figure shows that as the elevation change is diminished in trips, all of the calculations begin to produce similar values. The third trip from the right, highlighted by the red arrow, demonstrates that although the elevation loss in this trip is large it does not affect the overall tractive effort value of the trip. The elevation loss in this trip is gradual. A portion of the trip contains a very steep incline. The tractive power values produced on the incline balance the negative tractive power values that are obtained throughout the rest of the trip. Figure 15 shows the tractive effort calculations that were produced when I used Equation 2. It shows that Equation 2 produces values similar to Equation 1 values.

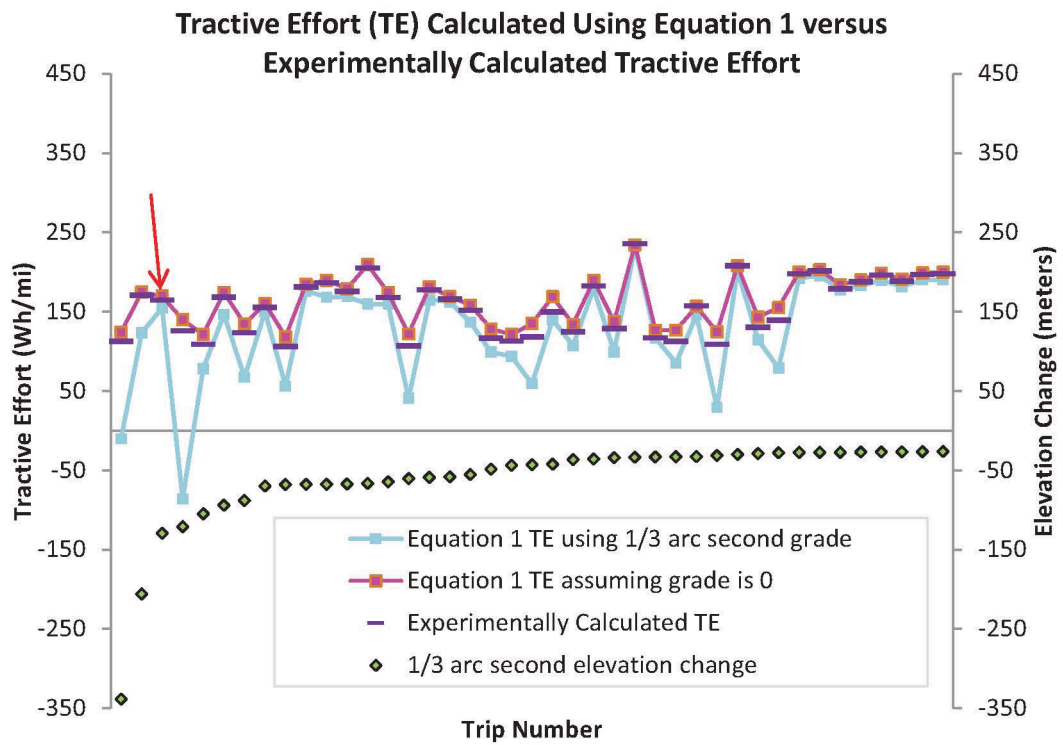


**Figure 14. Tractive effort values calculated using Equation 1 of the trips exhibiting large elevation loss. The data are plotted along the x-axis by trip number ordered by elevation change. The red arrow highlights a trip that contains a steep incline that negates the large elevation loss that occurs slowly across the rest of the trip.**

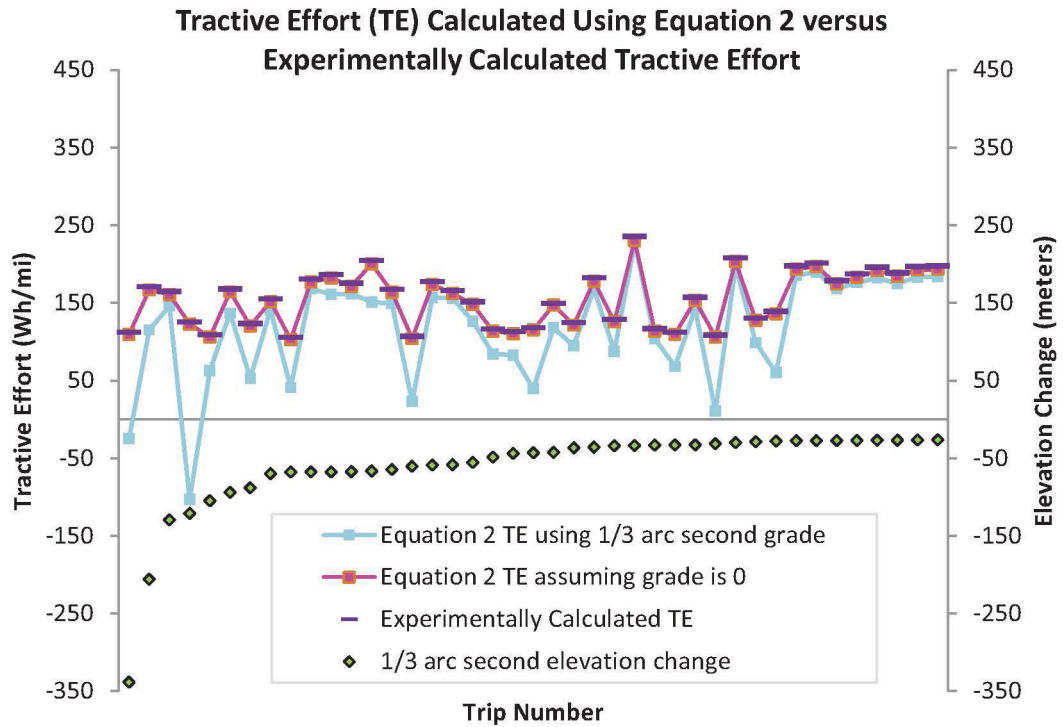
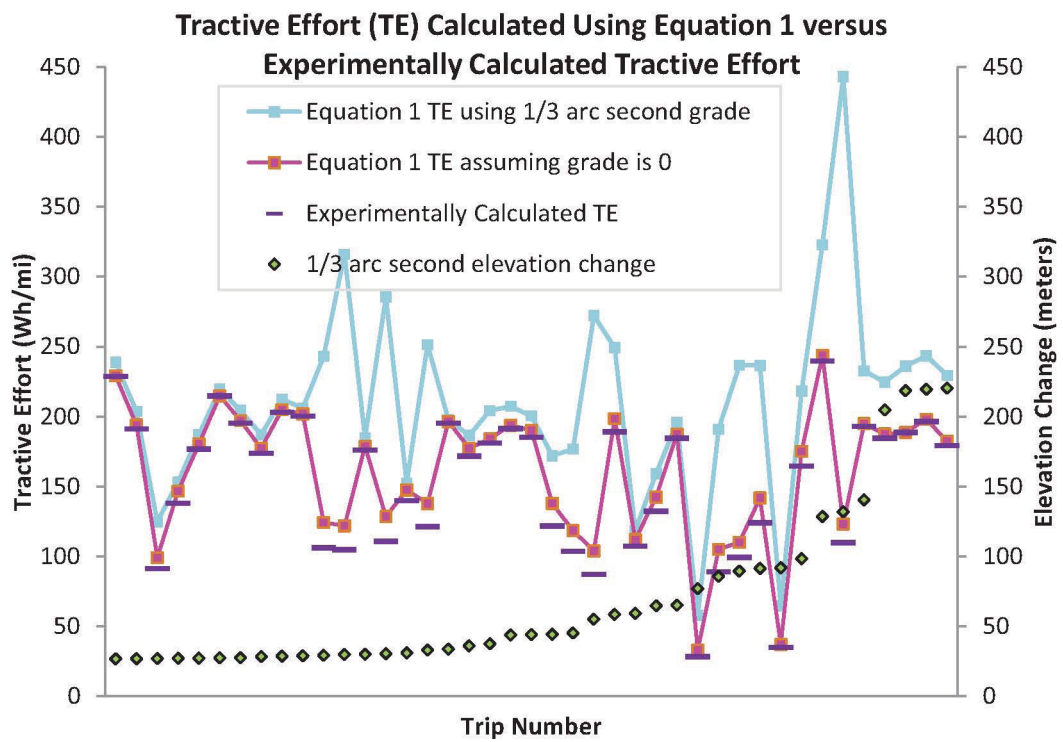


**Figure 15. Tractive effort values calculated using Equation 2 of the trips exhibiting large elevation loss. The data are plotted along the x-axis by trip number ordered by elevation change.**

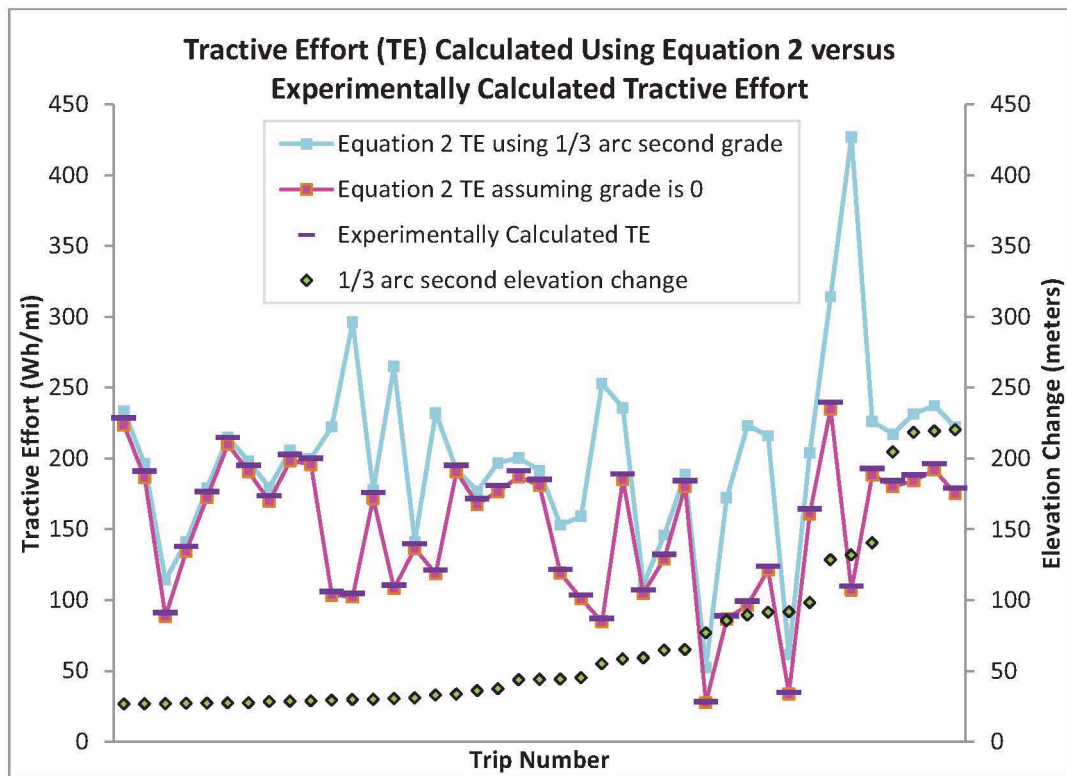
Figure 16 and Figure 17 show the trips that demonstrate the largest elevation gains. Figure 16 shows tractive effort values calculated using Equation 1. Figure 17 shows tractive effort values calculated using Equation 2. Both of these figures demonstrate that experimentally calculated tractive effort underestimates the tractive effort in trips that exhibit large elevation gain. Again, the tractive effort calculations using no grade track much closer to the experimentally calculated values.

Figure 18 and Figure 19 show trips where elevation gain is near zero. Figure 18 shows tractive effort values calculated using Equation 1. Figure 19 shows tractive effort values calculated using Equation 2. These two graphs show the greatest error in the calculations that use the 1/9-arc second grade. However, most of the values are close to the experimentally calculated values.





**Figure 16. Tractive effort values calculated using Equation 1 of the trips exhibiting large elevation gain. The data are plotted along the x-axis by trip number ordered by elevation change.**



**Figure 17.** Tractive effort values calculated using Equation 2 of the trips with the greatest elevation gain. The elevation change also is graphed for reference. The data are plotted in the order of elevation loss to gain.

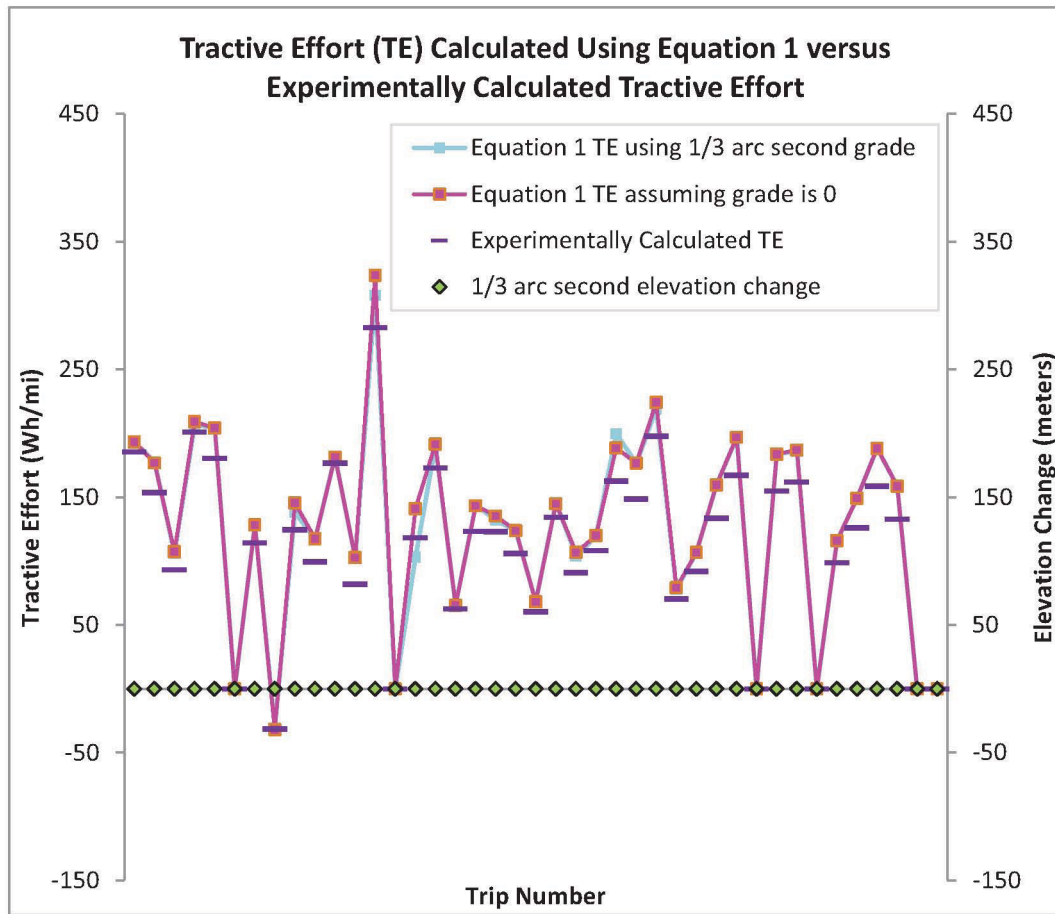


**Figure 18.** Tractive effort values calculated using Equation 1 of the trips consisting of little or no elevation change. The elevation change also is graphed for reference. The data are plotted in the order of elevation loss to gain.

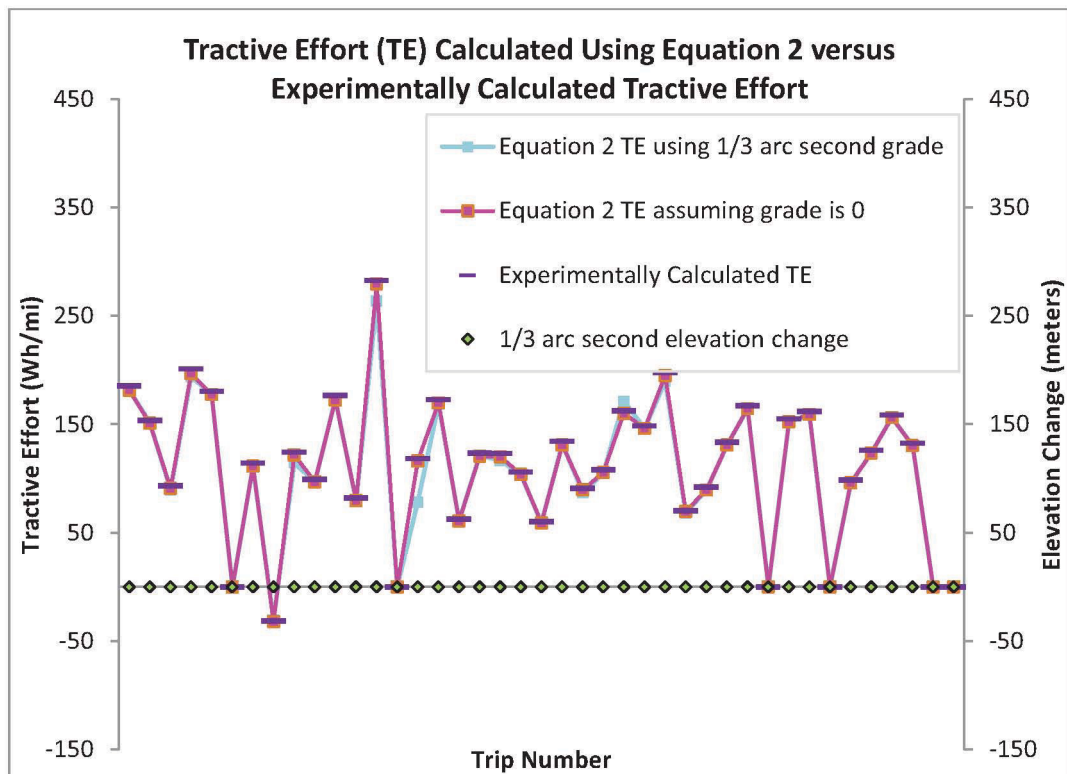


**Figure 19. Tractive effort values calculated using Equation 2 of trips consisting of little or no elevation change. The elevation change also is graphed for reference. The data are plotted in the order of greatest loss elevation loss to gain.**

A box and whisker chart of the experimentally calculated tractive effort values and the tractive effort values produced from Equation 2 using 1/3 arc second data is shown in Figure 20. The results are binned by miles per gallon. Ninety percent of the 1657 trips fall between 0 and 75 miles per gallon. Nearly half of the 1647 trips fall within the 25 - 50 mpg bin. In all three bins the range of outliers is greater in Equation 2 using 1/3 arc second grade.

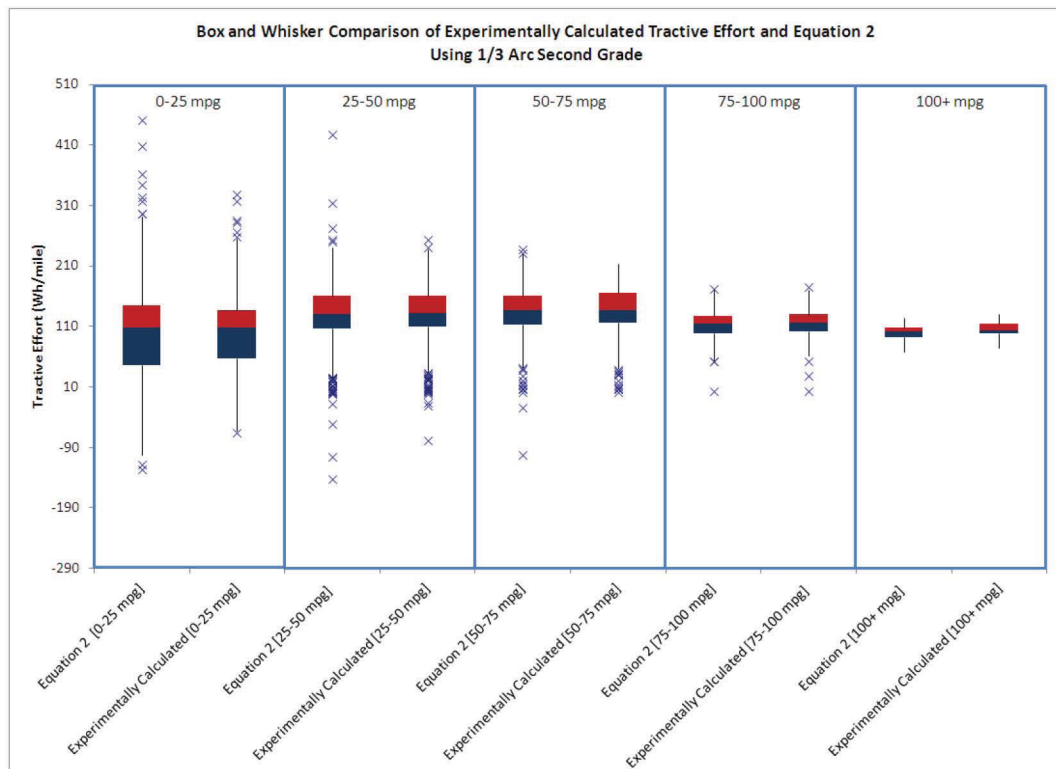


**Figure 20. Box and whisker chart comparing the distributions between tractive effort calculated experimentally and those calculated using Equation 2 and 1/3 arc second grade.**

All of the results shown above indicate that the experimentally calculated values do not consider road grade. In order to accurately characterize the driving intensity of a trip with a large change in elevation it is important to include grade.

#### 4.5: Differences between 1/3 and 1/9 Arc Second NED Data

The section above indicates that it is difficult to determine which source of elevation data is optimal. It would be ideal to show that the 1/3 arc second data can be used to produce good tractive effort results because the coverage of the 1/9 arc second data is very limited across the United States. Examination of the descriptive statistics of the two elevation datasets shows that there appears to be little difference. The statistics are shown in Table 3. This research does not use the altitude obtained from the GPS due to the inaccuracy shown in the table.



**Table 3. Descriptive statistics of the various sources of elevation.**

	<b>GPS Elevation (meters)</b>	<b>1/3-Arc Second Elevation (meters)</b>	<b>1/9-Arc Second Elevation (meters)</b>
<b>Maximum</b>	595	361	357
<b>Minimum</b>	-126	0	0
<b>Average Altitude</b>	14	16	16
<b>Standard Deviation</b>	25	22	22

The maximum change between two individual data points will provide a good example of a worst-case error. Figure 21, Figure 22, Figure 23 and Figure 24 show the trips with the largest instantaneous change in elevation. Figure 21 shows the elevation profile of Trip 1, which contains the largest instantaneous positive change in the 1/9-arc second elevation data. Figure 22 shows Trip 1's change in elevation. Figure 23 shows the profile of Trip 2, which contains the largest instantaneous positive change in the 1/3-arc second elevation data. Figure 24 shows Trip 2's change in elevation. In both cases, the dramatic change in elevation is caused by the GPS failing to transmit data for a large number of seconds.

Figure 21 and Figure 23 show that the 1/9-arc second data appear smoother and visually more representative of an actual road surface. However, when the results of these two trips are compared to the experimentally obtained data, they do not produce expected results.

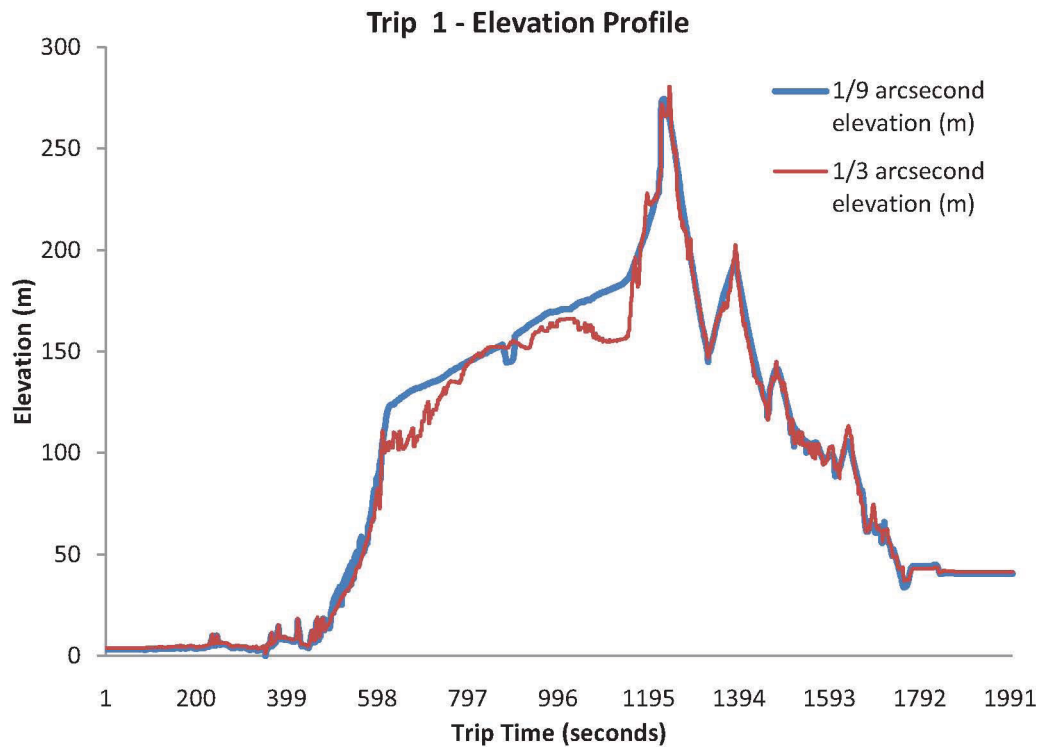


**Figure 21.** Trip 1 represents the single trip that had the greatest positive elevation change in the 1/9-arc second elevation dataset. These data are plotted along the x axis starting with the first elevation point collected to the last data point collected.

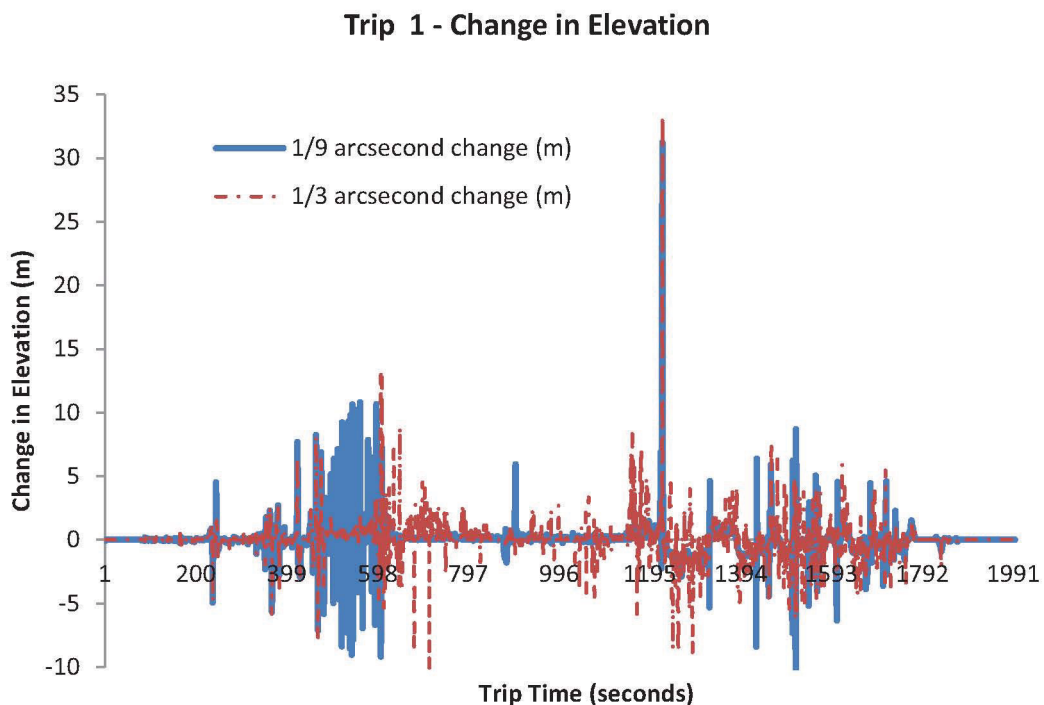


**Figure 22.** Trip 1 elevation change. This chart helps demonstrate the differences between the changes in elevation between the 1/9 and 1/3-arc second elevation datasets. These data are plotted in the order they were collected.

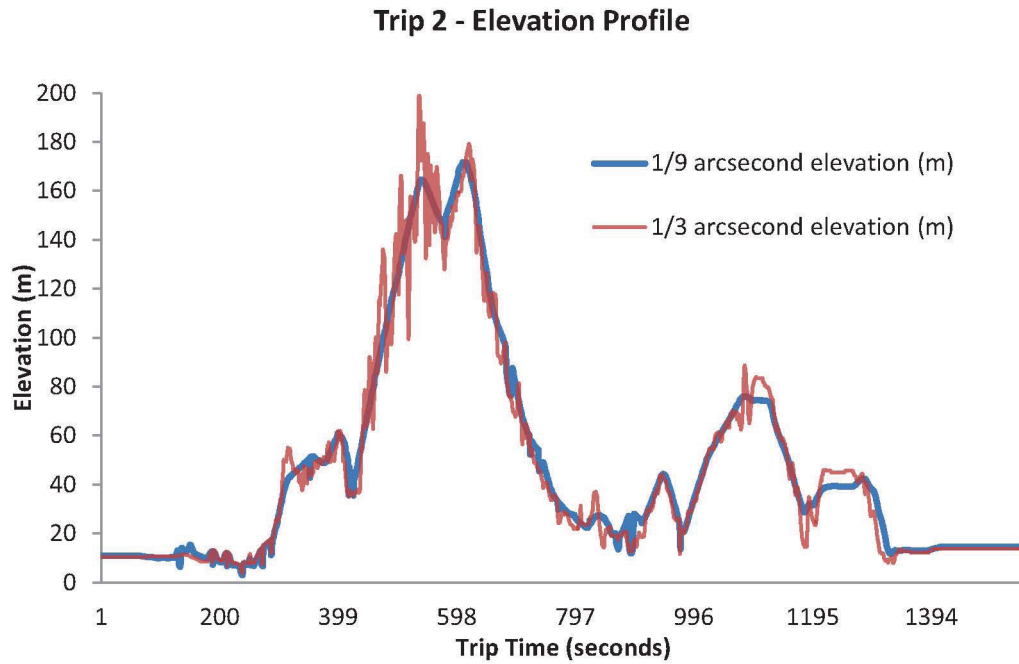


**Figure 23.** Trip 2 represents the single trip that had the greatest positive elevation change in the 1/3-arc second elevation dataset. These data are plotted in the order they were collected.

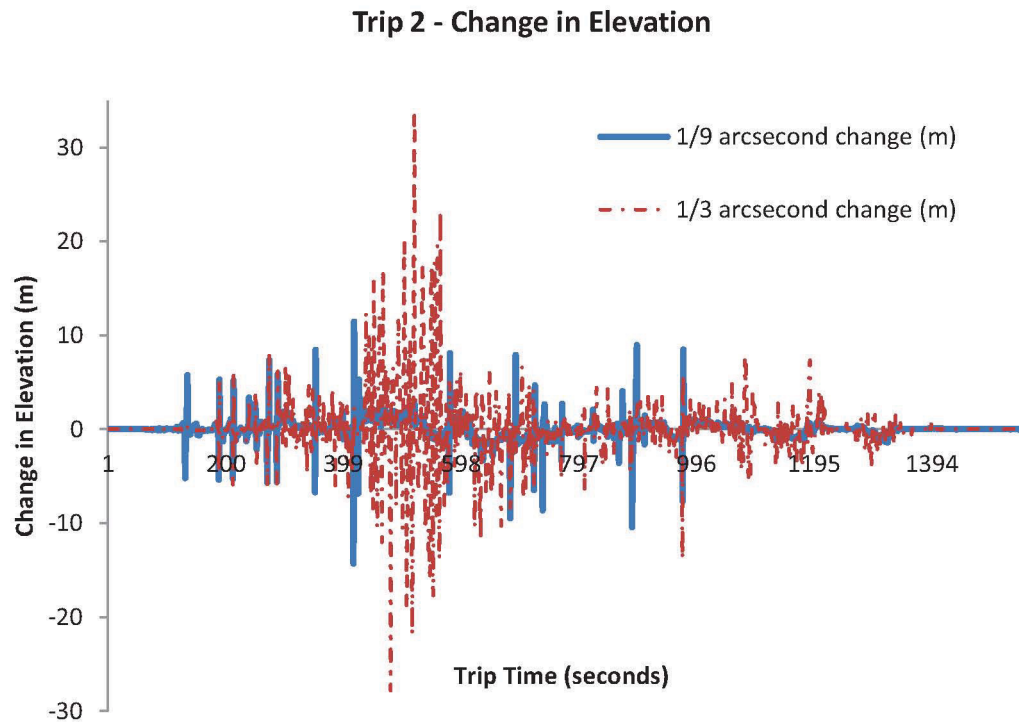


**Figure 24.** Trip 2 elevation change. This chart helps demonstrate the differences between the changes in elevation between the 1/9 and 1/3-arc second elevation datasets. These data are plotted in the order they were collected.

Table 4 shows that the elevation data with the greatest change do not appear to cause more inaccuracy in the tractive effort produced. This suggests that errors in the altitude do not necessarily change the accuracy of the aggressiveness calculations.

**Table 4. This table shows tractive effort results for both Trip 1 and Trip 2. In both cases, the results are counterintuitive. The results of the calculations using the elevation data that exhibit the greatest change are closest to the experimentally calculated value.**

<b>Elevation Data with the Greatest Change</b>	<b>Trip</b>	<b>Equation 1 Tractive Effort Using 1/9-Arc Second Data (Wh/mile)</b>	<b>Equation 1 Tractive Effort Using 1/3-Arc Second Data (Wh/mile)</b>	<b>Experimentally Calculated Tractive Effort</b>
1/9 arc second	Trip 1	189.762	204.311	181.039
1/3 arc second	Trip 2	182.585	181.152	179.682

I was unable to show which elevation source has a lower source of error. Practicality dictates that most research will have to use the 1/3-arc second elevation data because they are the most widely available. The research shows that road grade is mostly relevant in calculations with high elevation gain or loss. Figure 25 was produced to show the differences between tractive efforts calculated using the 1/3 arc second elevation and the 1/9 arc second elevation. For example, the pink series shows the difference between Equation 2 tractive efforts calculated using 1/3 arc second grade and 1/9 arc second grade. The gray bars show the difference between Equation 1 tractive efforts calculated using 1/3 arc second grade and 1/9 arc second grade. The figure shows that Equation 2 is less sensitive to the errors in elevation. The average error between the 1/3 arc second and 1/9 arc second calculations using Equation 2 is approximately 5 meters, whereas the average error using Equation 1 is approximately 19 meters. The largest error occurs on small trips that are less than 0.3 miles. It also shows that the delta

between the 1/3 and 1/9 grade data is smaller when Equation 2 is applied. These results indicate that Equation 2 is less sensitive to errors in elevation.

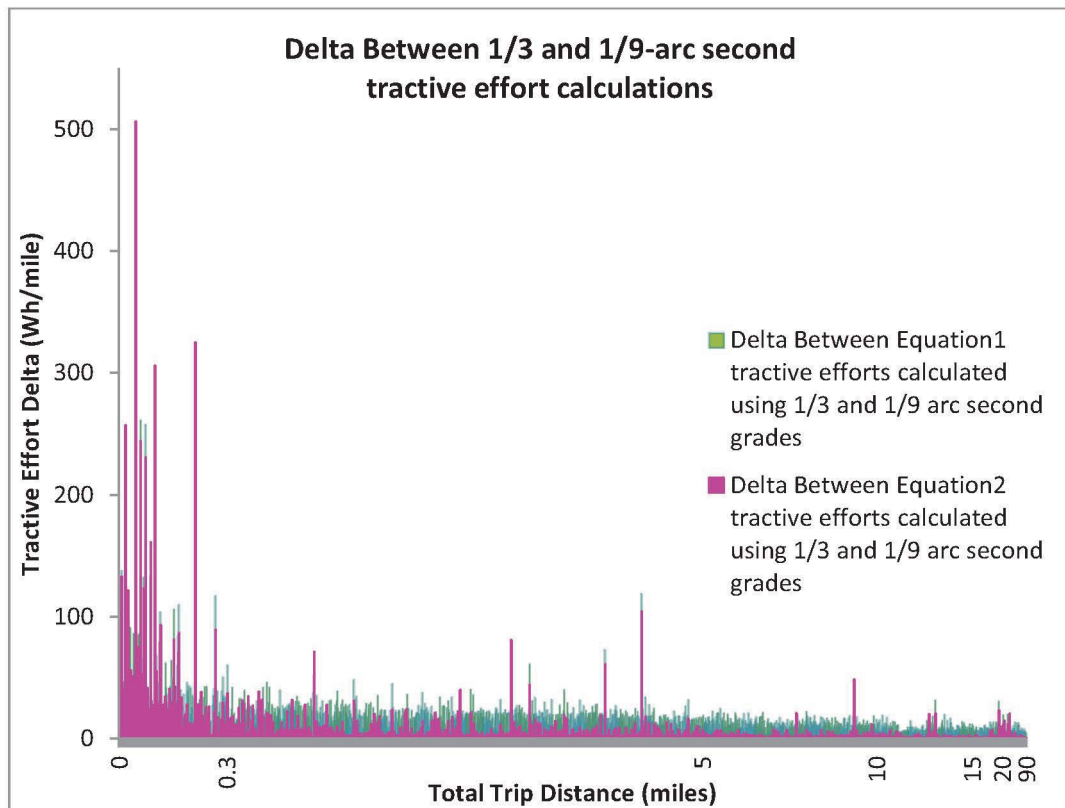


**Figure 25.** This graph shows the delta between the 1/3 and 1/9 arc second tractive effort values using both Equation 1 and Equation 2. The largest error between the two calculations occurs in trips that are less than 0.3 miles. The delta between the two tractive effort values is minimized when Equation 2 is used.



## **Chapter 5: Evaluation of the Effectiveness of Incorporating Geographic Road Type into a Route Type Algorithm**

Advancements in alternative fuel vehicle technology are driven by a requirement to produce more fuel-efficient vehicles that will reduce vehicle operating costs and reduce the environmental impact of transportation. Two basic metrics describing fuel economy are city mpg and highway mpg. Consumers are very familiar with these two metrics and frequently use them as a deciding factor when purchasing a vehicle.

EPA requires original equipment manufacturers to provide consumers both city and highway mpg metrics via the EPA window sticker. Until recently, EPA only required two dynamometer tests used to calculate the city and highway mpg metrics. The first test (the Urban Dynamometer Driving Schedule) is designed to simulate urban or city driving. The second test (the Highway Fuel Economy Test) is designed to simulate highway driving. These two tests are not robust enough to accurately model recent advancements in vehicle technology or current driving styles. The results of the two tests tend to overestimate fuel economy (Environmental Protection Agency 2006).

In 2006, EPA published a document detailing a new five-cycle method of fuel economy and emissions tests. They incorporated three additional dynamometer tests that increase the accuracy of the fuel economy values in hybrid electric vehicles by a 22.3% decrease in city mpg and a 12.9% decrease in highway mpg. In lieu of performing actual dynamometer tests, EPA provides an adjustment to the standard Urban Dynamometer Driving Schedule and Highway Fuel Economy Test produced values. This adjustment scales the fuel economy estimates closer to the results produced in the new five-cycle methodology

(Environmental Protection Agency 2006). Research performed by AVTA researchers showed that EPA's adjustment to the test results for the Hymotion PHEV Urban Dynamometer Driving Schedule and Highway Fuel Economy Test did not sufficiently match the on-road data published by AVTA (Gondor et al. 2009).

EPA has not published any research showing that they have considered intersecting drive data with road geography to improve or validate their metrics for highway and city drive cycles. They stated that they will not consider using on-road testing to provide values for city and highway fuel economy because on-road testing does not provide easily repeatable results (Environmental Protection Agency 2006).

### **5.1: Three Route Type Calculation Methods**

Because EPA required tests and adjustments do not provide a good fuel economy estimate for the Hymotion PHEV, engineers use other methods to estimate fuel economy. One source engineers use for route type calculations is the Society of Automotive Engineers' (SAE) Technical Standard J2841 (SAE 2010). This standard describes numerous methods for calculating PHEV route types. The simplest methodology described within Standard J2841 uses average speed to calculate route type. The standard recommends breaking the data up into two route types (i.e., city and highway), using an average speed. The average speed is chosen by cumulatively plotting the vehicle miles traveled versus the average trip speed. Next, researchers pick a percentage of trips that will occur in the city and a percentage that will occur on highways. The average value that lies in between the two percentages is chosen from the plot. The standard uses the common

assumption that 55% of the vehicle miles traveled will be urban driving and the other 45% will occur on the highway. However, each individual dataset should be analyzed to produce a threshold value that works (SAE 2010). This research uses the threshold value of 37 mph. This threshold value is used within other AVTA Hymotion PHEV algorithms. All trips with an average speed less than or equal to 37 mph are classified as city trips. All trips with average speeds higher than 37 mph are classified as highway trips.

In contrast, AVTA data analysis performed on the Hymotion PHEV Prius use a specific algorithm designed by AVTA engineers to classify route type. The AVTA algorithm uses average speed, vehicle stops, and vehicle accelerations to classify city and highway trips types.

The geographic route type classification uses the type of road that intersects each individual data point to provide a city or highway classification. The trips are analyzed for the percentage of highway and city roads they contain. The greater percentage is used as the route type.

## **5.2: Incorporating Geographic Road Type into Vehicle Trip Data**

The research process flow for the geographic road type classification is shown in Figure 26. ESRI StreetMap North America detailed streets data were used to provide the road types used in this research. The detailed street data are derived from 2005 Tele Atlas StreetMap Premium (ESRI 2010). I projected all of the geographic data layers to Web Mercator. This created a uniform data projection among all of the geographic datasets. The data produced by this research are intended for use in a web application. ESRI suggests using the Web Mercator projection for all data that will be served within a web application (ESRI

2010). The Web Mercator projection has a linear unit of meters. This allows all calculations made using this projection to produce a distance unit of meters.

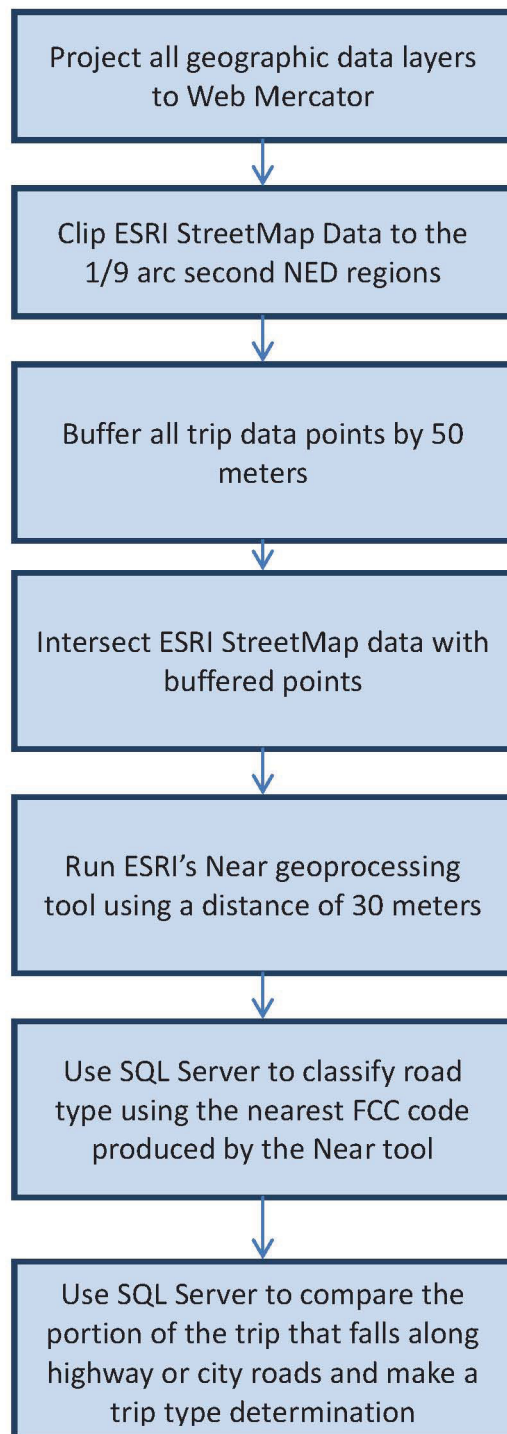
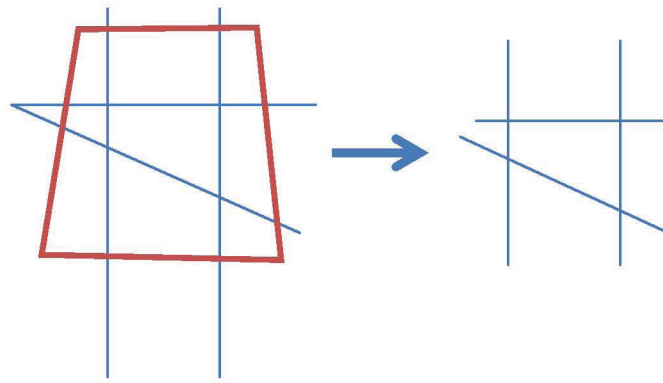


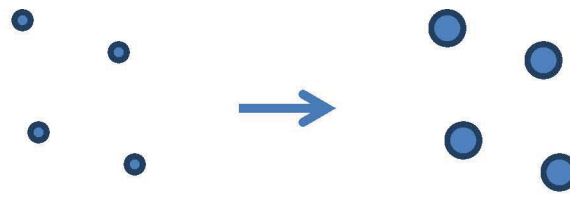
**Figure 26. Data flow of the highway and city geographic route type classification.**

The high resolution of ESRI StreetMap data makes it computationally expensive to work with. It can take minutes to display, zoom or pan the detailed StreetMap layer. Using the StreetMap Layer in ESRI ArcMap geoprocessing tools can cause the tools to take hours to finish. To create a more optimized subset of data, I used ESRI's Clip geoprocessing tool to produce a street layer only containing roads within the 1/9-arc second NED region polygons. Next, I used ESRI's Buffer geoprocessing tool to create a buffer of 50 meters around each trip data point, a distance large enough to account for the standard error produced by consumer-grade GPS units. Last, I used ESRI's Intersect geoprocessing tool to produce a layer containing only roads that intersected the buffered points. A diagram of this process is shown in Figure 27. Also, screenshots of the interfaces of all of the geoprocessing tools discussed here can be viewed in the Appendix E.

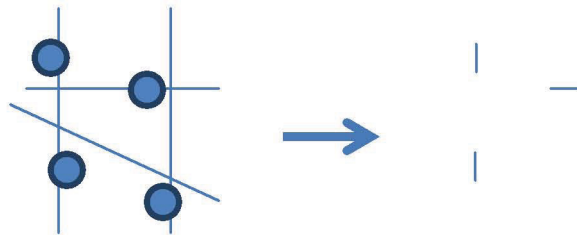




1 - Clip streets to polygon produces a subset of streets



2 - Buffer trip data points by 50 m produces trip points representing a larger surface area



3 - Intersect buffered trip data points with the clipped streets to produce a much smaller street data layer

**Figure 27. Provides an example of how the Clip, Buffer and Intersect geoprocessing tools create a small subset of street data.**

Next, I used ArcMap's Near geoprocessing tool. This tool provided a unique ID of the nearest road to the each trip data point. It also returned the distance from each trip data point to its nearest road. The unique ID was used to determine the feature class code (FCC) of the street nearest each point. The FCC provides a categorization of road types. A document produced by Geographic Data Technology, available on the California Department of Transportation website, was used to decode the FCC values (DOT 2011).

Originally, I used ESRI's classification of the FCC codes available within their thematic StreetMap layer provided with ArcMap 10 to classify road type as highway or city. The list of FCC codes and their respective ESRI classification are shown below in Table 5.

**Table 5. Feature class code classifications used in this research.**

<b>ESRI Road Classification</b>	<b>FCC Code</b>	<b>Road Type</b>	<b>Average Speed Calculated from Trip Data (kph)</b>	<b>Maximum Speed Calculated from Trip Data (kph)</b>
Major Highways	A10, 11, 12, 13, 14, 15, 16, 17, 18, 19	Highway	93	167
Highways	A20, 21, 22, 23, 24, 25, 26, 27, 28, 29	Highway	35	120
Major Roads	A30, 31, 32, 33, 34, 35, 36, 37, 38, 39	City	28	142
Local Traffic	A40, 41, 42, 43, 44, 45, 46, 47, 48, 49, 61	City	19	136
Other Ramps	A60	City	30	122
Traffic Circle	A62	City	4	50
Ramps	A63, 64	Highway	58	143
Other Thoroughfare	A70	City	35	123
Pedestrian	A71	City	34	125
Alley	A73	City	7	127

Microsoft SQL Server was used to classify each data point as being either city or highway using the following query:

```
Update SampleXYData Set RoadType = 'Highway'
Where FCC Like 'A1%' or FCC Like 'A2%' or FCC = 'A63' or FCC = 'A64'

Update SampleXYData Set RoadType = 'City'
Where FCC Like 'A4%' or FCC like 'A3%' or FCC = 'A62' or FCC = 'A61' or FCC = 'A75' or FCC = 'A73' or FCC = 'A74' or FCC = 'A60' or FCC = 'A70' or FCC = 'A71'
```

I initially classified FCC codes A63 and A64 as city. The results of this classification indicated that there was a misclassified road type. I produced a query that displayed each FCC code and its associated average speed, as shown in Table 5. The query showed that A63 and A64 produce very high average speeds. This indicated that they would be good candidates for highway classification. Figure 28 shows an example of a trip that was misclassified with A63 and A64 classified as city roads. It shows that a large portion of the roadways beneath the example trip are A63 and A64 road types. The trip shown in Figure 28 classified properly as a highway trip once the A63 and A64 classifications were changed to highway.

## FCC Codes A63 and A64

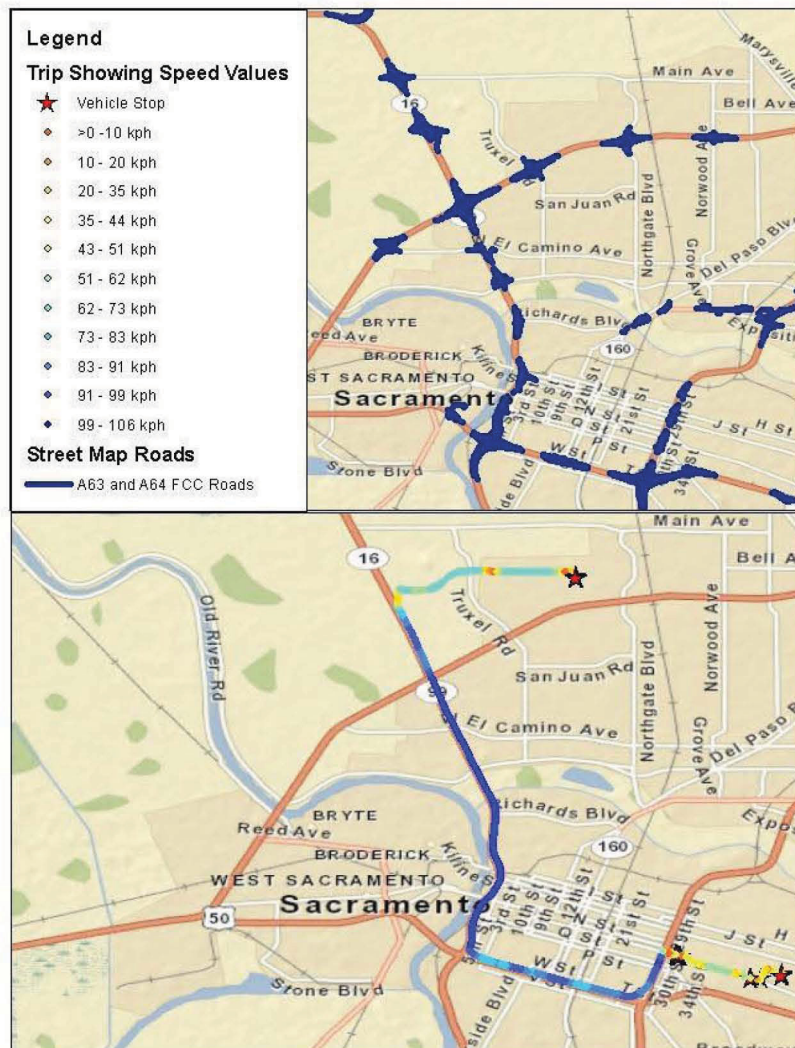


**Figure 28. Map showing a trip that was improperly classified as a city trip when the codes A63 and A64 were classified as city roads.**

Table 5 shows another potential error that arises during the geographic classification. It presents some points classified as pedestrian walkways and alleys. This type of error occurs because the trip point data were closer to a pedestrian walkway than they were to the roadway presumably being traveled on. This is possible due to the error introduced by consumer-grade GPS units. It is

highly unlikely that a vehicle would be traveling in a pedestrian walkway. The number of data points that produced this classification was small (approximately 0.07%). The alley classification comprised nearly 1% of the overall classified data. The alley classifications do not affect the results of the route type determination because they classify as city driving. The map in Figure 29 shows the trip with the single highest occurrence of alley street type classifications.

Next, I used Microsoft SQL Server to analyze each trip for its percentage traveled on highway roads and its percentage traveled on city roads. I updated the route type of the trip was updated to the type with the greatest percentage.



## Example Showing Possible Misclassification

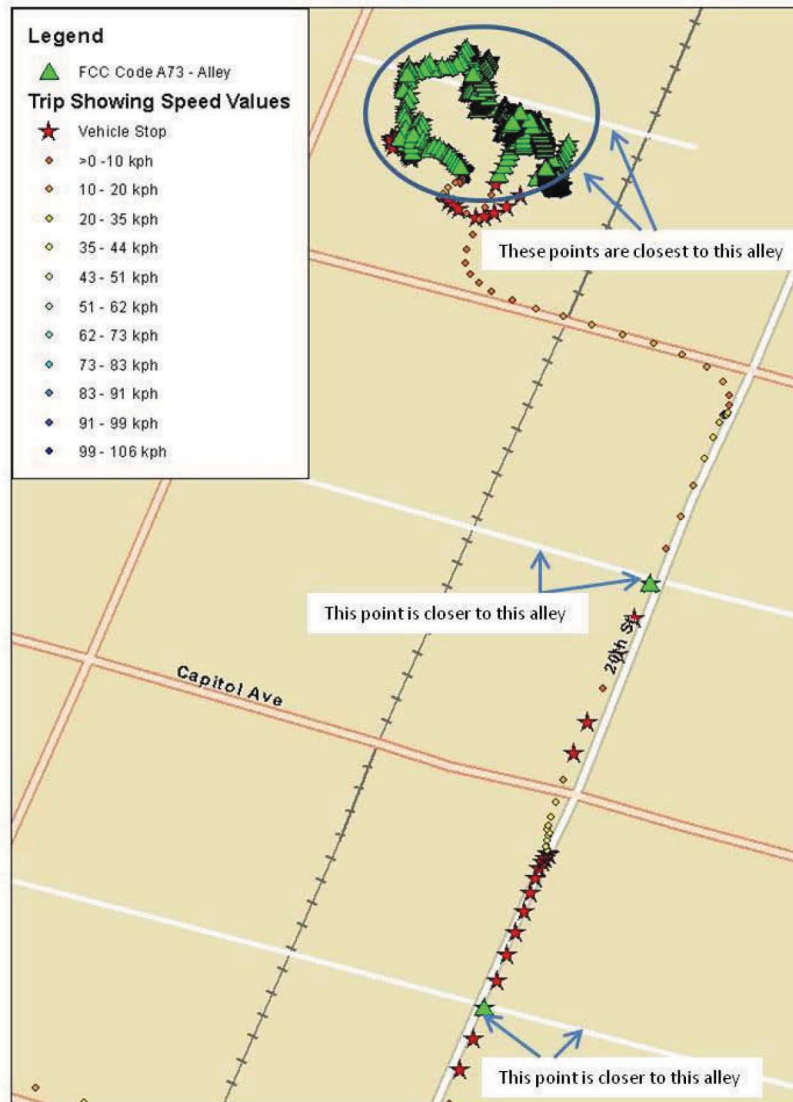


**Figure 29. Map demonstrating a trip that includes many alley road type classifications.**

### **5.3: Comparison of Geographically determined Route Type to J2841 and AVTA route types**

In order to understand the results of this research, it is necessary to understand the various operation modes of PHEVs. A PHEV is considered to be operating in charge-depleting (CD) mode when it is depleting the additional battery storage. Once the additional battery storage is depleted, the PHEV operates as a hybrid electric vehicle. This mode is called charge-sustaining (CS) mode. Long trips will likely produce a combination of both modes (called CD/CS mode). AVTA researchers have found that these modes make it difficult to adjust dynamometer test results to better approximate real world driving results (Gondor et al. 2009).

I compared the results of three different route type algorithms. One classification used the recommended SAE J2841 average speed algorithm (referred to herein as J2841). The second classification was the AVTA classification algorithm (referred to herein as AVTA). The third classification (referred to as GEO) was the classification performed by intersecting the road type with the trip data discussed in the research section above. The results of the research are shown in Table 6. Table 7 shows the differences between the GEO calculation and the AVTA and J2841 calculations. Figure 30 charts the results shown in Table 7.

**Table 6. Fuel economy results for all three classification algorithms.**

Route Type	Algorithm	Trip Category	mpg
City	AVTA	CS	37.38
City	GEO	CS	38.15
City	J2841	CS	38.47
City	AVTA	CD	55.18
City	GEO	CD	55.49
City	J2841	CD	55.72
City	AVTA	CD/CS	45.44
City	GEO	CD/CS	46.08
City	J2841	CD/CS	47.14
Highway	AVTA	CS	44.32
Highway	GEO	CS	44.73
Highway	J2841	CS	44.86
Highway	AVTA	CD	61.39
Highway	GEO	CD	62.81
Highway	J2841	CD	62.28
Highway	AVTA	CD/CS	53.41
Highway	GEO	CD/CS	54.58
Highway	J2841	CD/CS	53.26

**Table 7. Shows the delta between the miles per gallon calculations produced by the GEO algorithm and the J2841 and GEO calculations.**

Delta (GEO-AVTA) CS City	0.7712
Delta (GEO-J2841) CS City	-0.3221
Delta (GEO-AVTA) CD City	0.3035
Delta (GEO-J2841) CD City	-0.2374
Delta (GEO-AVTA) CD/CS City	0.6401
Delta (GEO-J2841) CD/CS City	-1.066
Delta (GEO-AVTA) CS Highway	0.4074
Delta (GEO-J2841) CS Highway	-0.1289
Delta (GEO-AVTA) CD Highway	1.414
Delta (GEO-J2841) CD Highway	0.5304
Delta (GEO-AVTA) CD/CS Highway	1.1705
Delta (GEO-J2841) CD/CS Highway	1.3241

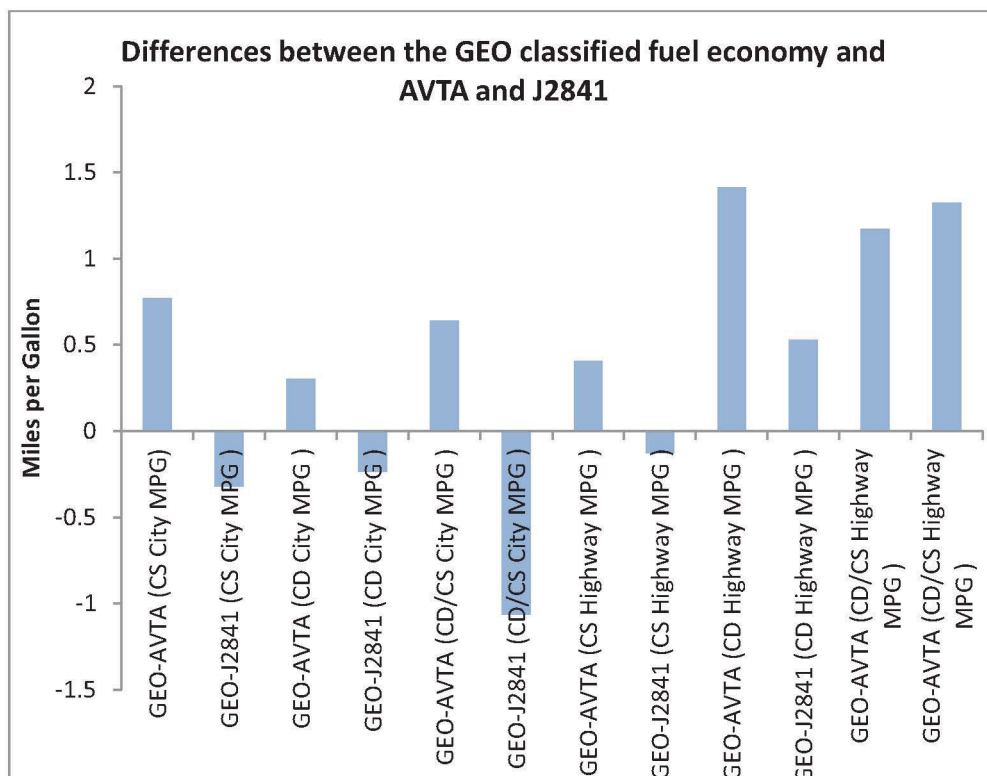


**Figure 30. Chart graphically displaying data showed in Table 7.**

The results show that the GEO route type algorithm works well. The largest difference shown in Figures 29 and 30 is in charge depleting highway trips and is 1.4 miles per gallon. The GEO algorithm can classify the fuel economy of any particular PHEV route type within approximately one mile per gallon. This is expected because the GEO algorithm is inherently speed based. Although it performs well, the GEO route type is error prone. This section discusses some potential errors that can arise when using the GEO route type algorithm.

Trips that occur on highways during rush hour or within construction zones resemble city driving. The GEO algorithm will incorrectly classify these types of trips because they occur mostly on highway road types. An example is shown in Figure 31.

## Example Showing Highway Trip During Rush Hour

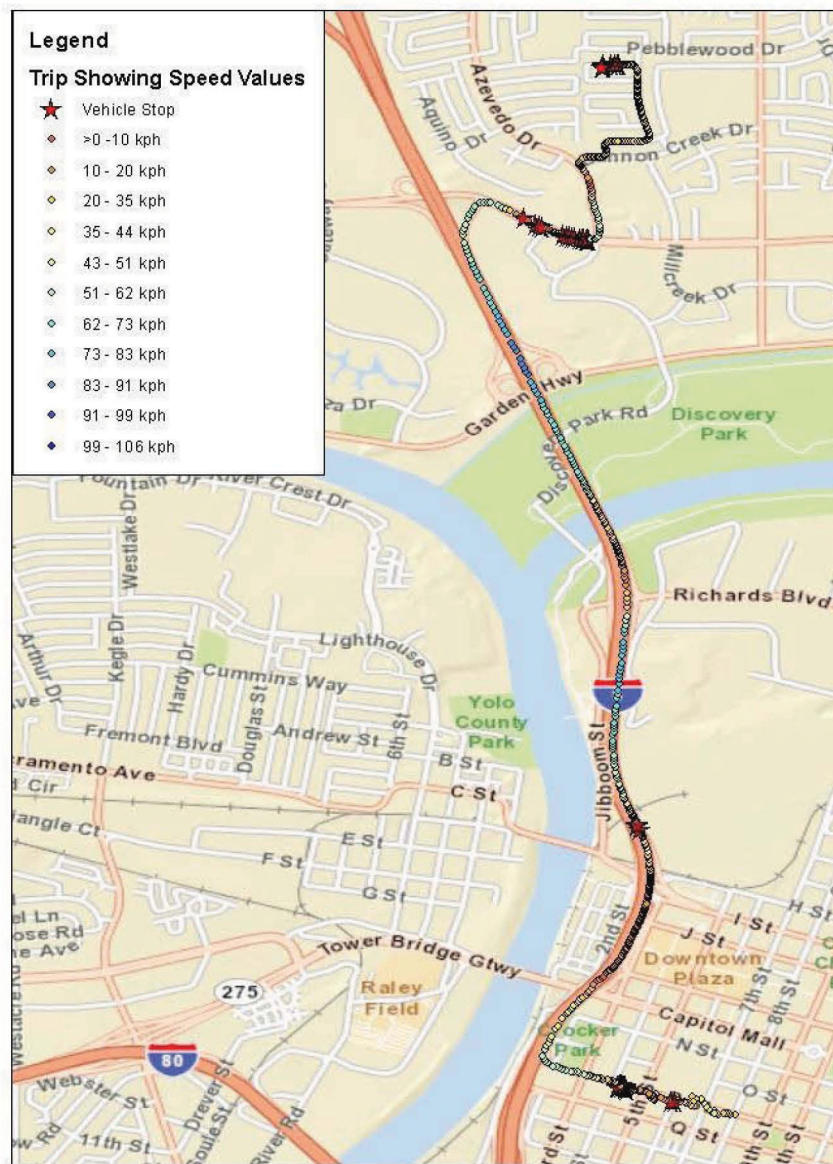


**Figure 31. Map showing a trip classified as highway by the GEO algorithm, but the trip is more representative of a city trip. It shows many lower speeds along the interstate and a few stops. There are portions of the trip where the speed approaches zero. This trip occurred around 4 p.m. on a weekday, indicating the trip likely occurred during rush hour.**



It is important to note that the GEO algorithm is not the only algorithm capable of producing errors. Figure 32 shows an example of how the J2841 calculation possibly misclassified a trip.

### Example Showing Average Speed Misclassification

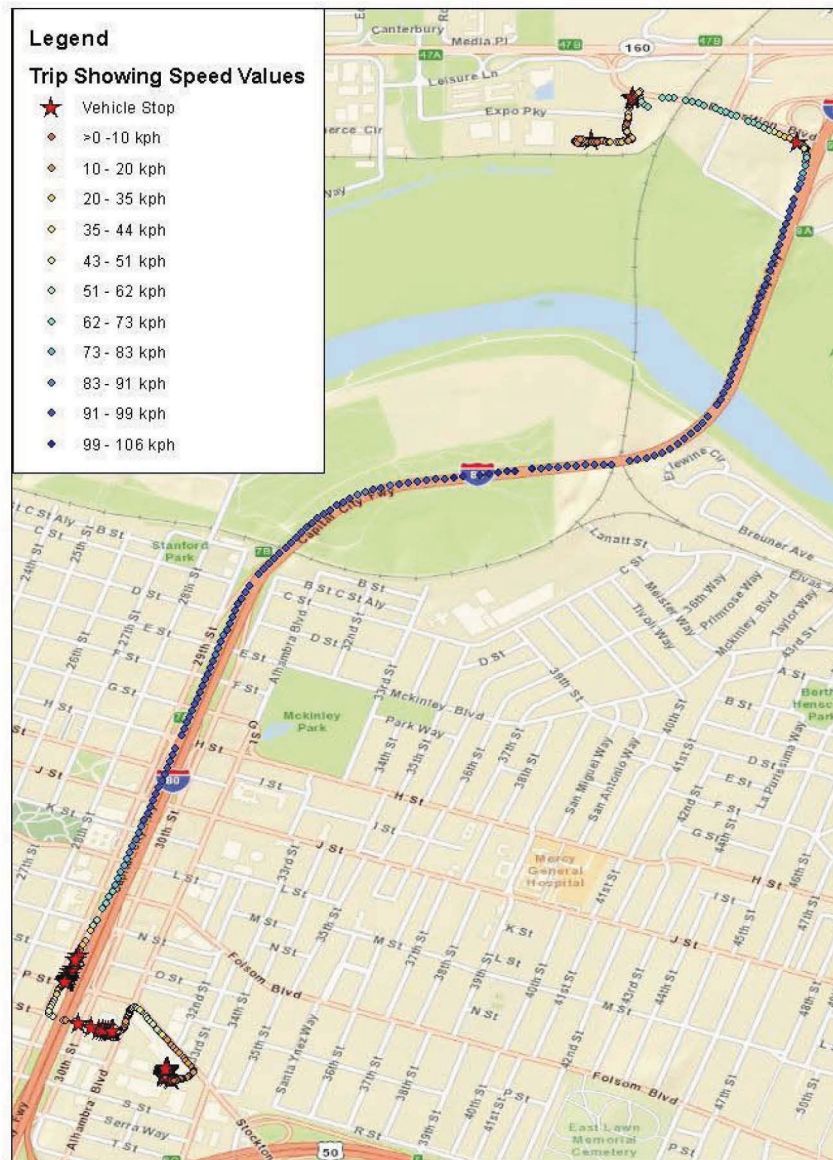


**Figure 32. An example of J2841 possibly misclassifying a trip. The majority of the trip occurs on an interstate over fast speeds. However, there are numerous stops at the beginning of the trip that may cause the average to inaccurately reflect the route type.**

Table 7 shows the differences between the calculations produced by each algorithm. Table 7 suggests that, in most cases, the GEO route type classification produces fuel economy values that are closer to the AVTA classification than those produced using J2841.

## **Chapter 6: Conclusions**

### **6.1: Incorporating Slope into Aggressiveness Calculations**

Chapter 4 discusses the incorporation of slope into standard driving intensity algorithms and details a methodology for obtaining road slope given latitude and longitude. It compared the results of two general tractive effort calculations to the results of the experimentally obtained tractive effort values. Hypothesis 1 was satisfied; I showed that the incorporation of road grade significantly changes the results of driving intensity calculations. The results demonstrated that tractive effort algorithms ignoring road slope overestimated driving intensity in trips exhibiting elevation loss by as much as 211 Wh/mile and underestimated driving intensity in trips exhibiting elevation gain by as much as 333 Wh/mile. In order to accurately characterize tractive effort in trips with large elevation gain or loss, it is necessary to incorporate road grade.

I also showed that Equation 2 is not as sensitive as Equation 1 to variances in elevation values between the 1/3 and 1/9 arc second datasets. Both 1/3 and 1/9 arc second data produced similar results when used with Equation 2. Also, trips with very short distances can produce large errors. This indicates that grade should not be used with very short trips.

This research did not study the error that could be introduced if the GPS fails to transmit data. If the GPS fails to transmit data for a significant period of time, the calculated grade may be incorrect. 1/9 arc second data appear to produce smoother elevation profiles. However, I was unable to definitively show that the 1/9 arc second elevation data are more accurate than the 1/3 arc second elevation

data. Future research should investigate the results achieved when SRTM data are used for obtaining elevations.

## **6.2: Using Geographic Road Type to Classify Route Type**

The research study presented in Chapter 5 provides a methodology for obtaining geographic road type given a latitude and longitude. It details how to use the geographic road type to classify the vehicle route type. Next, it compares the proposed geographic route type determination algorithms results to those of SAE J2841 and the AVTA route type algorithm.

This research did not completely prove Hypothesis 2. It is possible to classify the vehicle route type by only considering the geographic road type of a trip; however I showed examples in which it produced inaccurate classifications. Examination of the differences between the AVTA and GEO algorithms shows that the GEO algorithm is not as accurate as the AVTA calculation in determining route type. The GEO algorithm is insensitive to traffic conditions such as rush hour and construction. At the worst case, the GEO algorithm produced fuel consumption values that were accurate within 1.4 miles per gallon. Although this research showed that the GEO algorithm is not as accurate as the AVTA algorithm, it can be used to determine route type. The GEO route type appears to be more accurate than J2841, but J2841 is very simple to apply.

The method I proposed for obtaining the geographic route type is complex and requires human interaction during classification. Future research should consider ways to decrease the complexity of the classification and should compare the results produced by the GEO classification to other more complicated methods suggested within the SAE Technical Standard J2841.



### **6.3: Final Conclusions**

This thesis introduced the reader to the Advanced Vehicle Testing Activity and the research that it performs with regards to Plug-In Hybrid Electric Vehicles. I presented the relevant research to that has been conducted over the past 45 years. The research and results produced by incorporating geographic data into standard aggressiveness algorithms were discussed. Also, discussed were the results and research produced by using geographic road type to classify vehicle route type.

The research presented within this thesis provides methods for various interested entities to incorporate geographic data into algorithms containing a geographic component. Specifically it showed how to:

1. Obtain road slope given latitude and longitude.
2. Obtain geographic road type using vehicle latitude and longitude.
3. Determining a vehicle route type using geographic road data.

I demonstrated the effectiveness of incorporating geographic data into standard vehicle performance algorithms. It proved to be effective in the driving intensity algorithm and less effective in the route type determination. During my literature review I found that few vehicle technology research experts explore the effects of incorporating geographic data into their research. This is likely due to the difficulty of acquiring and working with geographic data. The methods used to acquire geographic data that I demonstrated in this thesis could be easily applied to other research problems.

## Chapter 7: References

- Arctur, D., and M. Zeiler. 2004. "Designing Geodatabases: Case Studies in GIS Data Modeling." *Redlands: ESRI Press*.
- AutoZone. 2012. "Glossary of Terms." 2012. Accessed March 21, 2012.  
<http://www.autozone.com/autozone/repairinfo/common/repairInfoMain.jsp?leftNavPage=glossary&startLetter=t&targetPage=glossarySelected>.
- Carlson, R., M. Duoba, T. Bohn, and A. Vyas. 2007. "Test and Analysis of Three Plug-In Hybrid Electric Vehicles." *SAE 2007 World Congress and Exhibition*.
- Carlson, R., J. Francfort, M. Shirk, and J. Smart. 2009a. "The Effect of Driving Intensity and Incomplete Charging on the Fuel Economy of a Hymotion Prius PHEV." *Idaho National Laboratory*.
- Carlson, R., L. Henning, M. Duoba, and S. Neeraj. 2009b. "Drive Cycle Fuel Consumption Variability of Plug-In Hybrid Electric Vehicles Due to Aggressive Driving." *SAE World Congress*, Detroit.
- Carlson, R., M. Shirk, and B. Gellar. 2010. "Factors that Impact the Fuel Consumption of Plug-In Hybrid Electric Vehicles." *The 25th World Battery, Hybrid and Fuel Cell Electric Vehicle Symposium & Exhibition*, Shenzhen, China.
- California DOT. 2011. "California Department of Transportation." *Geospatial Data Library*. Accessed September 2011.  
[http://www.dot.ca.gov/hq/tsip/gis/datalibrary/metadata/GDTdocs/FEATURE\\_CLASS\\_CODES-2000.PDF](http://www.dot.ca.gov/hq/tsip/gis/datalibrary/metadata/GDTdocs/FEATURE_CLASS_CODES-2000.PDF).
- Duoba, M., R. Carlson, F. Jehlik, J. Smart, and S. White. 2009. "Correlating Dynamometer Testing to In-Use Fleet Results of Plug-In Hybrid Electric Vehicles." *EVS 24*, Norway.
- Environmental Protection Agency. 2006. "Fuel Economy Labeling of Motor Vehicle Revisions to Improve Calculation of Fuel Economy Estimates." *Environmental Protection Agency Fuel Economy*. Accessed November 2011.  
<http://www.epa.gov/fueleconomy/420r06017.pdf>.
- ESRI. 2010a. "ESRI Data & Maps 10 White Paper." Accessed March 20, 2012.  
<http://www.esri.com/data/data-maps/J9974EsriDataandMaps10.pdf>.
- ESRI. 2010b. "Web Mercator The Standard for Sharing Data on the Web." Accessed September 2011.  
<http://www.esri.com/events/seminars/bettermaps/materials/pdfs/webmercator-smnr-brochure.pdf>.

- Evens, L., R. Herman, and T. Lam. 1976. "Multivariate Analysis of Traffic Factors Related to Fuel Consumption in Urban Driving." *Transportation Science* 10, No. 2: 205-215.
- Fang, Y., M. Friedman, G. Nair, M. Rys, and A. Schmid. 2008. "Spatial Indexing in Microsoft SQL Server 2008." *Proceedings of the 2008 ACM SIGMOD International Conference on Management of Data*, New York: ACM.
- Francfort, J., R. Carlson, M. Kirkpatrick, M. Shirk, J. Smart, and S. White. 2009. "Plug-in Hybrid Electric Vehicle Fuel Use Reporting Methods and Results." *INL Advanced Vehicle Testing Activity*. Accessed 2011. [http://avt.inl.gov/pdf/phev/phev\\_mpg\\_report\\_july09.pdf](http://avt.inl.gov/pdf/phev/phev_mpg_report_july09.pdf).
- Gillespie, T. 1992. "Fundamentals of Vehicle Dynamics." *Society of Automotive Engineers, Inc.*
- Gondor, J., A. Brooker, R. Carlson, and J. Smart. 2009. "Deriving In-Use PHEV Fuel Economy Predictions from Standardized Test Cycle Results." *5th IEEE Vehicle Power and Propulsion Conference*, Dearborn.
- GraphPad Software. 2005. "QuickCalcs t test calculator." Accessed March 10, 2010. <http://www.graphpad.com/quickcalcs/ttest1.cfm>.
- Green Gears. 2012. "Green Gears Blog." Accessed March 2012. <http://greengears.net/technical-stuff/v2green-system-installations/>.
- Gumusay, U., U. Alper, and A. Rukiye. 2008. "Use of Geographical Information Systems in Analyzing Vehicle Emissions: Istanbul as a Case Study." *International Archives of the Photogrammetry, Remote Sensing and Spatial Information Sciences XXXVII*: 997-1000.
- Idaho National Laboratory Advanced Vehicle Testing Activity. 2011. "North American Hymotion Prius PHEV Demonstration (V2Green data logger)." *Idaho National Laboratory Advanced Vehicle Testing Activity*. Accessed March 20, 2012. <http://avt.inl.gov/pdf/phev/HymotionPriusV2GreenApr08-Sept11.pdf>.
- Iu, H., and J. Smart. 2009a. "Determining PHEV Performance Potential - User and Environmental Influences on A123 System's Hymotion Plug-In Conversion Module for the Toyota Prius." *The 24th World Battery, Hybrid and Fuel Cell Electric Vehicle Symposium & Exhibition*, Stavanger, Norway.
- Iu, H., and J. Smart. 2009b. "Report on the Field Performance of the A123 Systems' Hymotion Plug-In Conversion Modeule for the Toyota Prius." *SAE World Congress*, Detroit.
- Kwon, J., J. Kim, E. Fallis, S. Pagerit, and A. Rousseau. 2008. "Impact of Drive Cycles on PHEV Component Requirements." *SAE 2008 International*, Warrendale: Society of Automotive Engineers.



- Larsen, G. 2009. "Calling a Web Service from within SQL Server." *Database Journal*. Accessed March 20, 2012. <http://www.databasejournal.com/features/mssql/article.php/3821271/Calling-a-Web-Service-from-within-SQL-Server.htm>.
- Lindenmaier, J., M. Stiegeler, and H. Kabza. 2009. "Data Acquisition Unit for Generation of Realistic Driving Cycles from Real World Data." *EVS 24*, Stavanger, Norway.
- McGuire, T., T. Roche, and A. Weinberger. 2008. "Analyzing Test Data from a Worldwide Fleet of Fuel Cell Vehicles at Daimler AG." *The Mathworks News and Notes*.
- Microsoft. 2011. "Definition and Explanation of a .DLL file." Accessed March 20, 2012. <http://support.microsoft.com/kb/87934>.
- Moran, K., B. Fastenrath, U. Foley, and J. Raimo. 2010. "Digital Maps, Connectivity, and Electric Vehicles - Enhancing the EV/PHEV Ownership Experience." *SAE Convergence*, Detroit: Society of Automotive Engineers, 76-83.
- Nam, E., C. Gierczak, and J. Butler. 2003. "A Comparison of Real-World and Modeled Emissions Under Conditions of Variable Driver Aggressiveness." *Power*.
- Nam, E., and R. Giannelli. 2005. *Fuel Consumption Modeling of Conventional and Advanced Technology Vehicles in the Physical Emission Rate Estimator (PERE)*. Technical Report, Assessment, and Standards Division Office of Transportation and Air Quality, U.S. Environmental Protection Agency.
- Office of Transportation and Air Quality. 2010. *Light-Duty Automotive Technology, Carbon Dioxide Emissions, and Fuel Economy Trends: 1975 Through 2010*. U.S. Environmental Protection Agency.
- Olken, F., and D. Rotem. 1986. "Simple Random Sampling from Relational Databases." *Proceedings of the Twelfth International Conference on Very Large Data Bases*, Kyoto, 160-169.
- ECEE. 2011. "Renewable Sources and Efficient Electrical Energy Systems." *ECEN2060*. Accessed March 21, 2012. [http://ecee.colorado.edu/~ecen2060/materials/lecture\\_notes/2060\\_HEV\\_1.pdf](http://ecee.colorado.edu/~ecen2060/materials/lecture_notes/2060_HEV_1.pdf).
- SAE. 2010. *Utility Factor Definitions for Plug-In Hybrid Electric Vehicles Using Travel Survey Data*. Society of Automotive Engineers Technical Standard.
- Smart, J., J. Francfort, D. Karner, M. Kirkpatrick, and S. White. 2009. "U.S. Department of Energy - Advanced Vehicle Testing Activity; Plug-In Hybride

Electric Vehicle Testing and Demonstration Activities." EVS24, Stavanger, Norway.

Stat Trek. 2011. "Sample Size: Simple Random Samples." Accessed June 2011.  
<http://stattrek.com/sample-size/simple-random-sample.aspx>.

Stricker, Nicole. 2008. "Factsheet: Plug-in hybrid vehicle demonstration." *Idaho National Laboratory Advanced Vehicle Testing Activity*. Accessed March 2012.  
[http://avt.inel.gov/pdf/phev/Seattle\\_PHEV\\_fact\\_sheet\\_12-15-08.pdf](http://avt.inel.gov/pdf/phev/Seattle_PHEV_fact_sheet_12-15-08.pdf).

USGS. 2010a. "Cumulous Portal for Geospatial Data." Accessed November 2011.  
<http://cumulus.cr.usgs.gov/services.php>.

USGS. 2010b. "Seamless Data Warehouse." Accessed March 20, 2012.  
<http://seamless.usgs.gov/>.

USGS. 2010c. "What is Elevation?" Accessed March 20, 2012.  
[http://seamless.usgs.gov/about\\_elevation.php](http://seamless.usgs.gov/about_elevation.php).



## Appendices

### Appendix A: C# Code used to create the User Defined Function for SQL Server

```
using System;
using System.Collections;
using System.Data;
using System.Data.SqlClient;
using System.Data.SqlTypes;
using Microsoft.SqlServer.Server;
using System.Xml;
using RetrieveElevationDataFromUSGS.elevationUSGS;

//used the article found here:
http://www.databasejournal.com/features/mssql/article.php/3821271/Calling-a-
Web-Service-from-within-SQL-Server.htm (Larsen 2009) to develop this
//create a sql server project within C# Visual Studio

public partial class UserDefinedFunctions
{
    //This sql function will return a table that will contain an elevation
    value
    [Microsoft.SqlServer.Server.SqlFunction(
        DataAccess = DataAccessKind.Read,
        FillRowMethodName = "GetAltitude_FillRow",
        TableDefinition = "elevation nvarchar(25)"
    )]

    public static IEnumerable GetAllElevations(string xlong, string ylat,
        string elevUnits, string sourceLayer, string elevationOnly)

    {
        Elevation_Service s = new Elevation_Service();
        s.Proxy = new System.Net.WebProxy("webbalance.inl.gov:8080");
        //send longitude, latitude, elevationUnits, sourceLayer, and
        elevationOnly parameters to the web service
        XmlNode retXML = s.getElevation(xlong, ylat, elevUnits, sourceLayer,
        elevationOnly);
        return retXML;
    }

    public static void GetAltitude_FillRow(object elevationObj, out
    SqlString elevation)
    {
        XmlNode n = (XmlNode)elevationObj;
        elevation = null;
        elevation = n.InnerText;
    }
};
```

## Appendix B: SQL Server T-SQL used to register the UDF .DLL File into the SQL Server Database

```
go
-- allows you to create external access CLR
-- also retrieved from
http://www.databasejournal.com/features/mssql/article.php/3821271/Calling-a-Web-Service-from-within-SQL-Server.htm (Larsen 2009)

ALTER DATABASE SeraThesisData SET TRUSTWORTHY ON;
GO

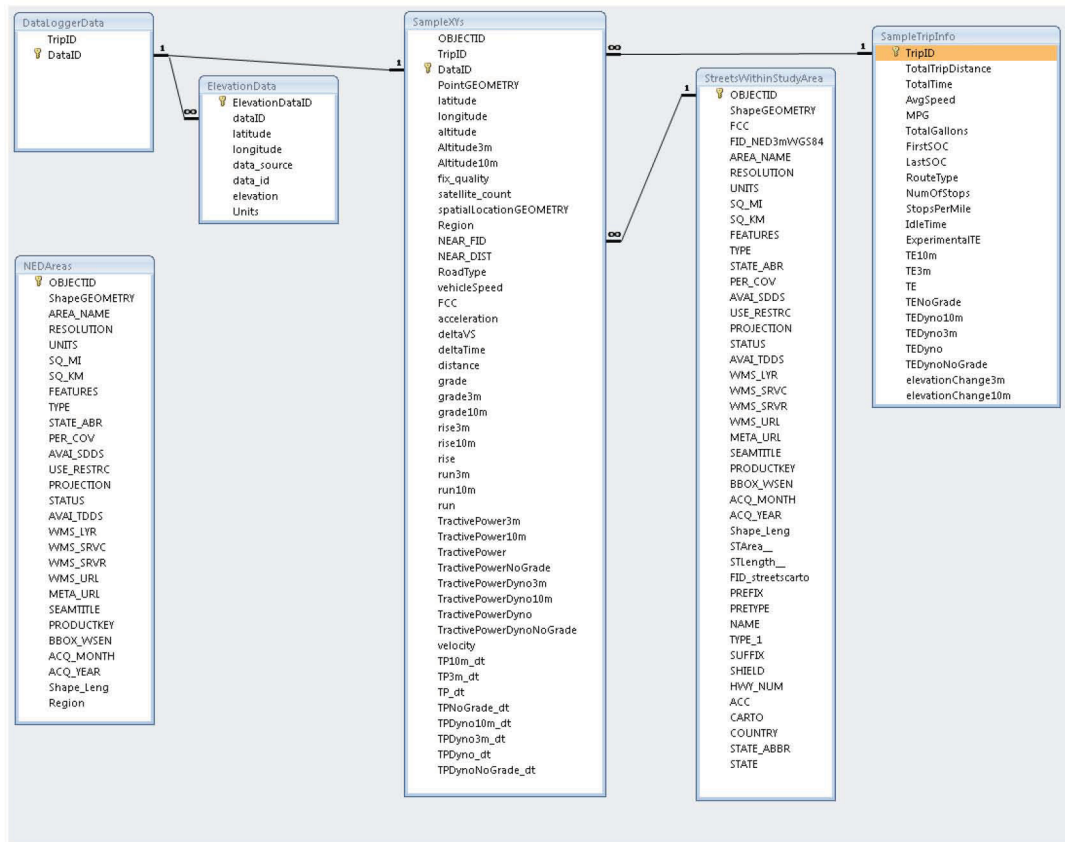
IF EXISTS (SELECT name FROM sysobjects WHERE name =
'GetAllElevations')
    DROP FUNCTION GetAllElevations
go
IF EXISTS (SELECT [name] FROM sys.assemblies WHERE [name] =
N'XmlSerializers')
    DROP ASSEMBLY [XmlSerializers]
IF EXISTS (SELECT name FROM sys.assemblies WHERE name =
'SqlClassLibrary')
    DROP ASSEMBLY SqlClassLibrary
GO

CREATE ASSEMBLY SqlClassLibrary FROM
'G:\SSIS\CLR\GetUSGSElevation\SqlClassLibrary.dll'
WITH PERMISSION_SET = External_Access

CREATE ASSEMBLY [XmlSerializers] from
'G:\SSIS\CLR\GetUSGSElevation\SqlClassLibrary.XmlSerializers.dll'
WITH permission_set = SAFE
GO

CREATE FUNCTION [dbo].[GetAllElevations](@xlong [nvarchar](4000),
@ylat [nvarchar](4000), @elevUnits [nvarchar](4000), @sourceLayer
[nvarchar](4000), @elevationOnly [nvarchar](4000))
RETURNS TABLE (
    [data_source] [nvarchar](500) NULL,
    [data_id] [nvarchar](100) NULL,
    [elevation] [nvarchar](25) NULL,
    [Units] [nvarchar](25) NULL
) WITH EXECUTE AS CALLER
AS EXTERNAL NAME
[SqlClassLibrary].[UserDefinedFunctions].[GetAllElevations]
```

## Appendix C: Entity Relationship Diagram for the SQL Server database used for the research presented within this thesis



### Notes:

- GEOMETRY Fields all have the term GEOMETRY proceeding the Field Name
- The only table linked from the original database is DataLoggerData. Because the information stored within this table is proprietary, all of the fields have been removed.
- All other fields were produced through the course of this thesis research
- NED Areas is the table produced from the region polygon obtained from USGS.
- StreetsWithinStudyArea is the table produced from the ESRI StreetMap USA detailed streets data layer.
- Throughout the research, I used 3m to refer to 1/9 arc second and 10m to refer to 1/3 arc second

## Appendix D: SQL Server T-SQL used to produce the random sample of trips used within the research presented within this thesis

```
-- =====
-- Author:          Sera White
-- Create date: 3/11/2011
-- Description:      Add a column to the table, fill it with values
--                   from the Rand() function, and select an ordered subset based on
--                   that new column.
-- The fundamental obstacle to using the Rand() function is that
-- Rand() is only evaluated once per query. The only way to assign a
-- different random number to every row in the table is to make a
-- separate assignment for each row, either when creating the row or
-- updating the table one row at a time:
-- This creates the table SampleTripInfo
-- =====
ALTER PROCEDURE [dbo].[uspAddRandomNumberToTripInfo]

AS
BEGIN
    -- SET NOCOUNT ON added to prevent extra result sets from
    -- interfering with SELECT statements.
    SET NOCOUNT ON;

    Select COUNT(TripID) From TripInfo
    Declare @counter as int = 1

    While @counter < 28992 begin

        Update TripInfo Set RandVal = Rand()*30000
        Where TripInfo.ObjectID = @counter

        set @counter = @counter + 1

    end
    Alter Table TripInfo Add RowID Int

    Update TripInfo Set RowID = tmp.calcVal
    From (Select TripID, ROW_NUMBER() Over (Order By RandVal) as
    calcVal From TripInfo) tmp Inner Join TripInfo On tmp.TripID =
    TripInfo.TripID

    Drop Table SampleTripInfo

    Select Top 1647 * Into SampleTripInfo From TripInfo Where
    InsideStudyArea = 1 Order By RowID

END
```

## Appendix E: Screenshots of Various ArcMap 10 Geoprocessing Tools

Buffer Geoprocessing Tool

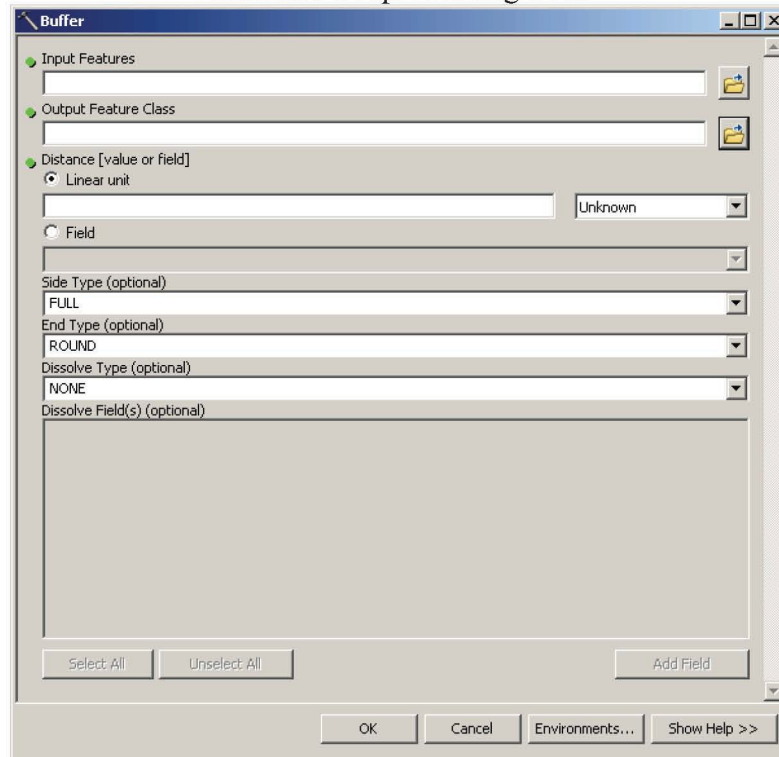
The Buffer Geoprocessing Tool dialog box is shown. It has a title bar with standard window controls. The main area contains several sections: 'Input Features' with a text box and a folder icon; 'Output Feature Class' with a text box and a folder icon; 'Distance [value or field]' with a radio button for 'Linear unit' (selected) and a text box, and a radio button for 'Field' with a text box; 'Side Type (optional)' with a dropdown menu set to 'FULL'; 'End Type (optional)' with a dropdown menu set to 'ROUND'; 'Dissolve Type (optional)' with a dropdown menu set to 'NONE'; and 'Dissolve Field(s) (optional)' with a large text box. At the bottom, there are buttons for 'Select All', 'Unselect All', and 'Add Field'. The bottom-most row contains 'OK', 'Cancel', 'Environments...', and 'Show Help >>' buttons.

Clip Geoprocessing Tool

The Clip Geoprocessing Tool dialog box is shown. It has a title bar with standard window controls. The main area contains several sections: 'Input Features' with a text box and a folder icon; 'Output Feature Class' with a text box and a folder icon; 'Distance [value or field]' with a radio button for 'Linear unit' (selected) and a text box, and a radio button for 'Field' with a text box; 'Side Type (optional)' with a dropdown menu set to 'FULL'; 'End Type (optional)' with a dropdown menu set to 'ROUND'; 'Dissolve Type (optional)' with a dropdown menu set to 'NONE'; and 'Dissolve Field(s) (optional)' with a large text box. At the bottom, there are buttons for 'Select All', 'Unselect All', and 'Add Field'. The bottom-most row contains 'OK', 'Cancel', 'Environments...', and 'Show Help >>' buttons.



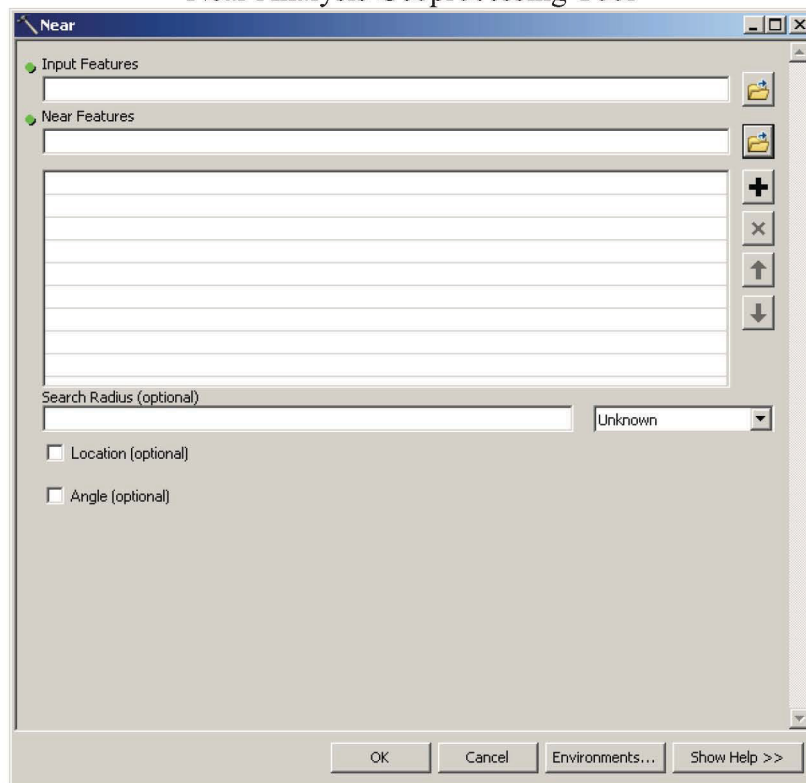
## Intersect Geoprocessing Tool



The Buffer tool dialog box is titled "Buffer". It contains the following fields and options:

- Input Features:** A text box with a browse button (folder icon).
- Output Feature Class:** A text box with a browse button (folder icon).
- Distance [value or field]:**
  - ☒ **Linear unit:** A text box and a dropdown menu currently set to "Unknown".
  - ☐ **Field:** A text box.
- Side Type (optional):** A dropdown menu set to "FULL".
- End Type (optional):** A dropdown menu set to "ROUND".
- Dissolve Type (optional):** A dropdown menu set to "NONE".
- Dissolve Field(s) (optional):** A large empty text area.
- Buttons:** "Select All", "Unselect All", and "Add Field" are located below the Dissolve Field(s) area.
- Footer:** "OK", "Cancel", "Environments...", and "Show Help >>" buttons.

## Near Analysis Geoprocessing Tool



The Near tool dialog box is titled "Near". It contains the following fields and options:

- Input Features:** A text box with a browse button (folder icon).
- Near Features:** A text box with a browse button (folder icon).
- Search Radius (optional):** A text box and a dropdown menu currently set to "Unknown".
- Location (optional):** An unchecked checkbox.
- Angle (optional):** An unchecked checkbox.
- Buttons:** A vertical stack of buttons (+, x, up arrow, down arrow) is located to the right of the Near Features text box.
- Footer:** "OK", "Cancel", "Environments...", and "Show Help >>" buttons.

## Appendix F: Free Body Diagram Detailing Physics Behind Equation 1

Consider a vehicle accelerating up a road sloped at an angle  $\alpha$  as shown in Fig. 1. The vehicle propulsion must generate a total force (i.e. “traction effort”)  $F_v$  to overcome aerodynamic drag ( $F_d$ ), rolling resistance ( $F_r$ ) and gravity ( $F_g$ ), and  $F_a$  to accelerate,

$$F_v = F_d + F_r + F_a + F_g = \frac{1}{2} \rho C_d A_v v^2 + f_{rr} M_v g \cos \alpha + M_v \frac{dv}{dt} + M_v g \sin \alpha, \quad (1.1)$$

where:

- $\rho$  air density = 1.204 kg/m<sup>3</sup> at 20°C, 1 atm
- $C_d$  aerodynamic drag coefficient
- $A_v$  vehicle frontal surface area (in m<sup>2</sup>)
- $v$  vehicle speed (in m/s)
- $M_v$  vehicle mass, i.e. weight (in kg)
- $g$  gravity = 9.81 m/s<sup>2</sup>
- $f_{rr}$  rolling resistance coefficient, or coefficient of rolling friction, typically 0.01 for car tires on concrete or asphalt
- $\sin \alpha \approx \tan \alpha = H/L = \text{road grade } Z \text{ (for small } \alpha \text{)}$
- $\cos \alpha \approx 1 \text{ (for small } \alpha \text{)}$

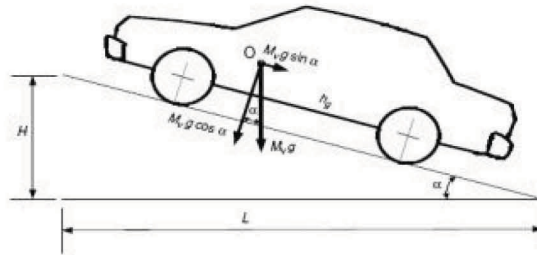


Figure 1: Vehicle ascending a road with grade  $Z = H/L$ .

The required traction power is

$$P_v = F_v v \approx \frac{1}{2} \rho C_d A_v v^3 + f_{rr} M_v g v + M_v v \frac{dv}{dt} + M_v g Z v. \quad (1.2)$$

NOTE: This figure and text were taken from ECEN 2060 Hybrid and Electric Vehicles Course Notes (Renewable Sources and Efficient Electrical Energy Systems 2011).